Roles of WO$_x$ on Pt/γ-Al$_2$O$_3$ catalysts on the prevention of Pt metal sintering during hydrogenolysis of glycerol to 1,3-propanediol

Miss Poonnapa Limsoonthakul

จุฬาลงกรณ์มหาวิทยาลัย
CHULALONGKORN UNIVERSITY

A Thesis Submitted in Partial Fulfillment of the Requirements
for the Degree of Master of Engineering in Chemical Engineering
Department of Chemical Engineering
FACULTY OF ENGINEERING
Chulalongkorn University
Academic Year 2019

บทบาทของทังสเตนออกไซด์บนตัวเร่งปฏิกิริยา Pt/γ-Al$_2$O$_3$ ในการป้องกันการเกิดซินเทอร์ของโลหะ
แพลทตินัมขณะทำปฏิกิริยาไฮโดรจิโนไลซิสของกลีเซอรอลเป็น 1,3-โพรเพนไดออล

น.ส.ปุณณภา ลิ้มสุนทรากูล

วิทยานิพนธ์นี้เป็นส่วนหนึ่งของการศึกษาตามหลักสูตรปริญญาวิศวกรรมศาสตรมหาบัณฑิต
สาขาวิชาวิศวกรรมเคมี ภาควิชาวิศวกรรมเคมี
คณะวิศวกรรมศาสตร์ จุฬาลงกรณ์มหาวิทยาลัย
ปีการศึกษา 2562

Thesis Title	Roles of WO$_x$ on Pt/γ-Al$_2$O$_3$ catalysts on the prevention of Pt metal sintering during hydrogenolysis of glycerol to 1,3-propanediol
By	Miss Poonnapa Limsoonthakul
Field of Study	Chemical Engineering
Thesis Advisor	Professor PIYASAN PRASERTHDAM, Ph.D.
Thesis Co Advisor	SUPAREAK PRASERTHDAM, Ph.D.

Accepted by the FACULTY OF ENGINEERING, Chulalongkorn University in Partial Fulfillment of the Requirement for the Master of Engineering

.... Dean of the FACULTY OF
ENGINEERING
(Professor SUPOT TEACHAVORASINSKUN, Ph.D.)

THESIS COMMITTEE

.... Chairman
(RUNGTHIWA METHAAPANON, Ph.D.)

.... Thesis Advisor
(Professor PIYASAN PRASERTHDAM, Ph.D.)

.... Thesis Co-Advisor
(SUPAREAK PRASERTHDAM, Ph.D.)

.... Examiner
(Professor SUTTICHAI ASSABUMRUNGRAT, Ph.D.)

.... External Examiner
(Assistant Professor Okorn Mekasuwandumrong, Ph.D.)

ปุณณภา ลิ้มสุนทรากูล : บทบาทของทังสเตนออกไซด์บนตัวเร่งปฏิกิริยา Pt/**γ**-Al$_2$O$_3$ ในการป้องกันการเกิดซินเทอร์ของโลหะแพลทตินัมขณะทำปฏิกิริยาไฮโดรจิโนไลซิสของกลีเซอรอลเป็น 1,3-โพรเพนไดออล. (Roles of WO$_x$ on Pt/**γ**-Al$_2$O$_3$ catalysts on the prevention of Pt metal sintering during hydrogenolysis of glycerol to 1,3-propanediol) อ.ที่ปรึกษาหลัก : ศ. ดร.ปิยะสาร ประเสริฐธรรม, อ.ที่ปรึกษาร่วม : ดร.ศุภฤกษ์ ประเสริฐธรรม

ปฏิกิริยาไฮโดรจิโนไลซิสของกลีเซอรอลเป็น 1,3-โพรเพนไดออล ถือเป็นปฏิกิริยาหนึ่งที่เปลี่ยนกลีเซอรอลที่มากเกินพอจากกระบวนการผลิตไบโอดีเซลให้เป็นผลิตภัณฑ์มูลค่าเพิ่มโดยเฉพาะ 1,3-โพรเพนไดออล ตัวเร่งปฏิกิริยาที่นิยมใช้สำหรับการผลิต 1,3-โพรเพนไดออล คือ ตัวเร่งปฏิกิริยาแพลทินัมบนตัวรองรับแกมมาอลูมินาที่สังเคราะห์ด้วยวิธีการเคลือบฝังแบบเปียก แม้ว่าปฏิกิริยาไฮโดรจิโนไลซิสของกลีเซอรอลจะเกิดขึ้นภายใต้อุณหภูมิ 140 องศาเซลเซียสและความดันไฮโดรเจน 5 บาร์ แต่ก็พบการเสื่อมสภาพของตัวเร่งปฏิกิริยาที่ไม่ผ่านการปรับสภาพ เทคนิคที่นำมาวิเคราะห์เพื่อศึกษาการเสื่อมสภาพของตัวเร่งปฏิกิริยานี้ เช่น การดูดซับทางกายภาพด้วยไนโตรเจน อินดัคทีพลีคัพเพิลพลาสมา การเลี้ยวเบนของรังสีเอ็กซ์และเทคนิคการโปรแกรมอุณหภูมิเพื่อทดสอบการเกิดออกซิเดชัน เป็นต้น จากการศึกษาพบการเสื่อมสภาพของตัวเร่งปฏิกิริยา คือ การหลุดออกของโลหะ การซินเทอร์ของโลหะและการเกิดโค้กบนตัวเร่งปฏิกิริยาขณะทำปฏิกิริยาในตัวเร่งปฏิกิริยาทั้งสองชนิด ได้แก่ แพลทินัม/แกมมาอลูมินาและแพลทินัม/ทังสเตนออกไซด์/แกมมาอลูมินา โดยทังสเตนออกไซด์สามารถป้องกันการหลุดออกของโลหะแพลทินัมและลดการเกิดโค้กบนผิวของตัวเร่งปฏิกิริยา และการมีทังสเตนออกไซด์บนตัวเร่งปฏิกิริยาแพลทินัม/ทังสเตนออกไซด์/แกมมาอลูมินายังเพิ่มประสิทธิภาพการเปลี่ยนกลีเซอรอลให้จำเพาะกับการเกิด 1,3-โพรเพนไดออลมากกว่า 1,2-โพรเพนไดออล ทั้งยังเพิ่มความมีเสถียรภาพของตัวเร่งปฏิกิริยาแพลทินัม/ทังสเตนออกไซด์/แกมมาอลูมินาให้ดีกว่าตัวเร่งปฏิกิริยาแพลทินัม/แกมมาอลูมินา โดยระบุได้ด้วยค่าการลดลงของการเปลี่ยนกลีเซอรอลในตัวเร่งปฏิกิริยาที่ผ่านการเร่งปฏิกิริยาไฮโดรจิโนไลซิสของกลีเซอรอล ดังนั้นการเติมทังสเตนออกไซด์บนตัวเร่งปฏิกิริยาแพลทินัม/แกมมาอลูมินาทำให้มีประสิทธิภาพในการเร่งปฏิกิริยา ค่าการเลือกเกิดของ 1,3-โพรเพนไดออล และความมีเสถียรภาพที่มากกว่า

สาขาวิชา   วิศวกรรมเคมี   ลายมือชื่อนิสิต ....

ปีการศึกษา   2562   ลายมือชื่อ อ.ที่ปรึกษาหลัก ....

                                         ลายมือชื่อ อ.ที่ปรึกษาร่วม ....

6170216521 : MAJOR CHEMICAL ENGINEERING

KEYWORD: Hydrogenolysis, Glycerol, 13-Propanediol, Platinum, Tungsten, Alumina, Deactivation, Leaching, Sintering, Coking

Poonnapa Limsoonthakul : Roles of WO_x on Pt/γ-Al_2O_3 catalysts on the prevention of Pt metal sintering during hydrogenolysis of glycerol to 1,3-propanediol. Advisor: Prof. PIYASAN PRASERTHDAM, Ph.D. Co-advisor: SUPAREAK PRASERTHDAM, Ph.D.

Hydrogenolysis of glycerol to produce 1,3-propanediol is the most effective reaction which conversing excess glycerol from biodiesel production to high-value-add product; especially, 1,3-propanediol. A solid catalyst which generally used as selective to 1,3-propanediol production is Pt-based catalyst with γ-Al_2O_3 supporter which was prepared by wet impregnation method in this study. Although hydrogenolysis of glycerol reaction has been carried out under mild conditions: 140 ℃ and 5 bar of initial H_2 pressure, the deactivation of non-reduced Pt/γ-Al_2O_3 catalyst is observed. To investigate the deactivation of the catalyst, the used Pt/γ-Al_2O_3 and Pt/WO_x/γ-Al_2O_3 catalysts were characterized by N_2-physisorption, ICP-OES, SEM-EDX, XRD, Py-IR, TPO and FTIR. In this study, deactivations are leaching, sintering and coke formation on both Pt/γ-Al_2O_3 and Pt/WO_x/γ-Al_2O_3 catalyst during the hydrogenolysis of glycerol in liquid phase. WO_x can hinder the sintering of Pt metal and retard the coke formation on the catalyst surface. Furthermore, the existence of WO_x on Pt/WO_x/γ-Al_2O_3 catalysts can also improve catalytic activity for glycerol conversion. Moreover, Pt/WOx/γ-Al_2O_3 catalysts can significantly increase the selectivity of 1,3-propanediol beyond 1,2-propanediol. Nevertheless, the stability of Pt/WO_x/γ-Al_2O_3 catalyst is better than that of Pt/γ-Al_2O_3 catalyst indicated by lower conversion drop of the used catalyst after the first hydrogenolysis of glycerol. Consequently, the addition of WO_x on Pt/γ-Al_2O_3 catalyst makes appropriated Pt-based catalyst performing in hydrogenolysis of glycerol in terms of higher activity, the selectivity of wanted 1,3-propanediol and stability of the catalyst.

Field of Study:	Chemical Engineering	Student's Signature	....
Academic Year:	2019	Advisor's Signature	....
		Co-advisor's Signature	....

ACKNOWLEDGEMENTS

TABLE OF CONTENTS

LIST OF TABLES

จุฬาลงกรณ์มหาวิทยาลัย

CHULALONGKORN UNIVERSITY

LIST OF FIGURES

CHAPTER I

INTRODUCTION

1.1 Introduction

The increment of fossil fuel usage has affected the creation of pollutant emission, especially carbon dioxide (CO_2), which encourages the greenhouse effect leading to the problem of global warming nowadays[1]. To alleviate CO_2 production, the exploration of alternative fuel source replacing the primitive fossil fuel has been needed[2]. Recently, biomass, the product derived from a living organism, has gained more attention for employing as an alternative feedstock in many applications such as biochemical and bioenergy because the biomass is ample in agricultural products. Hence, utilizing biomass is not only produced green products without generating pollutants that directly impact to environment but also added the value of low-cost agricultural materials[3].

In the past few decades, bioenergy means biofuels, consist of bioethanol and biodiesel, which the productions have been rapidly developed[4]. For biodiesel which provides wider applications of the vehicle system, it can be produced from triglycerides derived from plants such as palm, peanut, sunflower, soybean, jatropha[5], and rapeseed[1], constituting approximately 10 wt.% of total biomass[6]. Moreover, the triglycerides are also harvested from animal fat[7] and waste cooking oil[8]. Normally, triglyceride can be reached with short-chain alcohols, via transesterification reaction[9]. To produce ester compound and glycerol as main and byproduct, respectively. After that, the produced ester compound can be purified before employed as biodiesel in the next step[10].

In 2018, the global production of biodiesel was significantly increased by around 5%. From overall biodiesel production around the world, the top five countries accounted for 53% of global production. Most of them, Europe is the largest producer of biodiesel by region. Furthermore, the current leading country producers for biodiesel production are the United States (17%), Brazil (13%), Indonesia (10%), Germany (8%), and Argentina (5%), respectively[11].

In the future, biodiesel production trends to continuously enhanced around 4.5% annually to reach 41 billion liters in 2022, as shown in Figure 1.
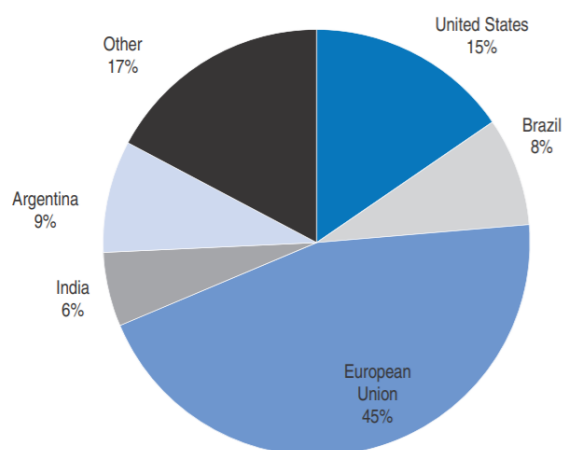
Figure 1 Country shares of biodiesel production in 2022[12]

However, the increment of biodiesel production affects the over excess glycerol storage, which is the byproduct during biodiesel production. Over generation of glycerol byproduct leads to the low-cost of glycerol in the chemical market. However, it is well known that glycerol is an important reactant for producing other chemical precursors.

To transform glycerol to other chemicals, the hydrogenolysis reaction of glycerol is the most basic approach which a highly effective catalyst plays an important role in terms of reactivity of glycerol conversion and selectivity of wanted 1,3-propanediol production. From the many kinds of highly effective catalysts that are available in the market, Pt-based catalyst has been recently reported as the most popular catalyst due to its high reactivity on hydrogenolysis reaction. However, the improvement of selectivity of wanted 1,3-propanediol production is still a challenge.

To improve the selectivity of 1,3-propanediol on Pt-based catalyst, the addition of tungsten oxide (WO_x) has been reported as an effective dopant to increase the selectivity of 1,3-propanediol production and enhance the catalytic reactivity because the existence of WO_x assists stabilization of the secondary

carbocation which is the crucial intermediate during the transformation of glycerol to 1,3-propanediol[13].

Although a combination of Pt and WO_x on γ-Al_2O_3 surface can improve the selectivity of 1,3-propanediol beyond 1,2-propanediol, deactivation of the catalyst by metal leaching, metal sintering, and coke formation is still difficult to avoid. Hence, understanding of deactivation on Pt/WO_x/γ-Al_2O_3 catalyst during hydrogenolysis of glycerol needed to design a better catalytic system for hydrogenolysis of glycerol to yield 1,3-propanediol.

Thereby, deactivation of clean Pt and Pt/WO_x, which are supported by γ-Al_2O_3, are focused during the hydrogenolysis of glycerol to 1,3-propanediol. Moreover, the effect of WO_x doping to prevent deactivation on Pt-based catalyst improving the catalytic performances in terms of activity, selectivity, and stability on hydrogenolysis of glycerol. The role of additional promoters such as WO_x is also investigated.

1.2 Objective

To investigate the role of WO_x on Pt/γ-Al_2O_3 catalyst to prevent deactivations from leaching and sintering of Pt metal as well as coke formation during hydrogenolysis of glycerol to 1,3-propanediol under low temperature and pressure (mild reaction conditions)

1.3 The Scopes of Research

The details of this research are shown below.

1.3.1 Studying the catalytic reaction for fresh and used catalysts through hydrogenolysis of glycerol at low temperature and pressure conditions (140 $^\circ$C and 5 bar of initial H_2 pressure)

1.3.2 Studying deactivation of Pt-based catalyst during hydrogenolysis process (Pt leaching, Pt sintering, and coke formation)

1.3.3 Studying the effect of WO_x on preventing catalytic deactivation of Pt-based catalyst

1.3.4 Studying catalytic stability in terms of recycle catalyst in hydrogenolysis process

1.4 Research Methodology

```
        Pt/γ-Al₂O₃                                    Pt/WOₓ/γ-Al₂O₃
            │                                               │
            ▼                                               ▼
┌──────────────────────────────┐        ┌──────────────────────────────┐
│ Dried γ-Al₂O₃ overnight at    │        │ Prepared 10 wt.% of WOₓ/γ-    │
│ 110 °C and calcined at 900 °C │        │ Al₂O₃ via wet impregnation    │
│ for 3 h                       │        │ method                        │
└──────────────────────────────┘        └──────────────────────────────┘
            │                                               │
            ▼                                               ▼
┌──────────────────────────────┐        ┌──────────────────────────────┐
│ Prepared 5 wt.% of Pt/γ-      │        │ Dried overnight at 110 °C and │
│ Al₂O₃ using wet impregnation  │        │ calcined at 900 °C for 3 h    │
│ method                        │        │                               │
└──────────────────────────────┘        └──────────────────────────────┘
            │                                               │
            ▼                                               ▼
┌──────────────────────────────┐        ┌──────────────────────────────┐
│ Dried overnight at 110 °C and │        │ Prepared 5 wt.% of Pt/WOₓ/γ-  │
│ calcined at 300 °C for 3 h    │◄───────│ Al₂O₃ by wet impregnation     │
│                               │        │ method                        │
└──────────────────────────────┘        └──────────────────────────────┘
```

Dried γ-Al$_2$O$_3$ overnight at 110 $^{\circ}$C and calcined at 900 $^{\circ}$C for 3 h

Prepared 10 wt.% of WO$_x$/γ-Al$_2$O$_3$ via wet impregnation method

Prepared 5 wt.% of Pt/γ-Al$_2$O$_3$ using wet impregnation method

Dried overnight at 110 $^{\circ}$C and calcined at 900 $^{\circ}$C for 3 h

Dried overnight at 110 $^{\circ}$C and calcined at 300 $^{\circ}$C for 3 h

Prepared 5 wt.% of Pt/WO$_x$/γ-Al$_2$O$_3$ by wet impregnation method

Characterization

- N$_2$ Physisorption
- Inductively coupled plasma (ICP)
- Scan Electron Microscope (SEM)
- X-ray Diffraction (XRD)
- FTIR adsorbed pyridine (Py-IR)
- Temperature Programmed Oxidation (TPO)
- Fourier-transform infrared spectroscopy (FTIR)

Reaction study

Discussion

Conclusion

CHAPTER II

BACKGROUND AND LITERATURE REVIEWS

The general information of glycerol and the hydrogenolysis of glycerol to 1,3-propanediol and other possible chemicals are mentioned in this section. Finally, the interesting catalysts and literatures, including definitions of sintering and coking, are reviewed with this chapter.

2.1 Glycerol

Currently, there are several methods to synthesize glycerol into other useful products, such as hydrolysis, saponification, and transesterification of fatty acid or vegetable oil. The applications of glycerol are illustrated in Figure 2, for example, pharmaceutical, cosmetic, food beverage, and chemical application.

Figure 2 Glycerol industrial applications[14]

Glycerol is a functional chemical compare with the other hydrocarbons. Accordingly, a large quantity of higher value-added products can be produced via different chemical reactions, as showed in Figure 3[15].
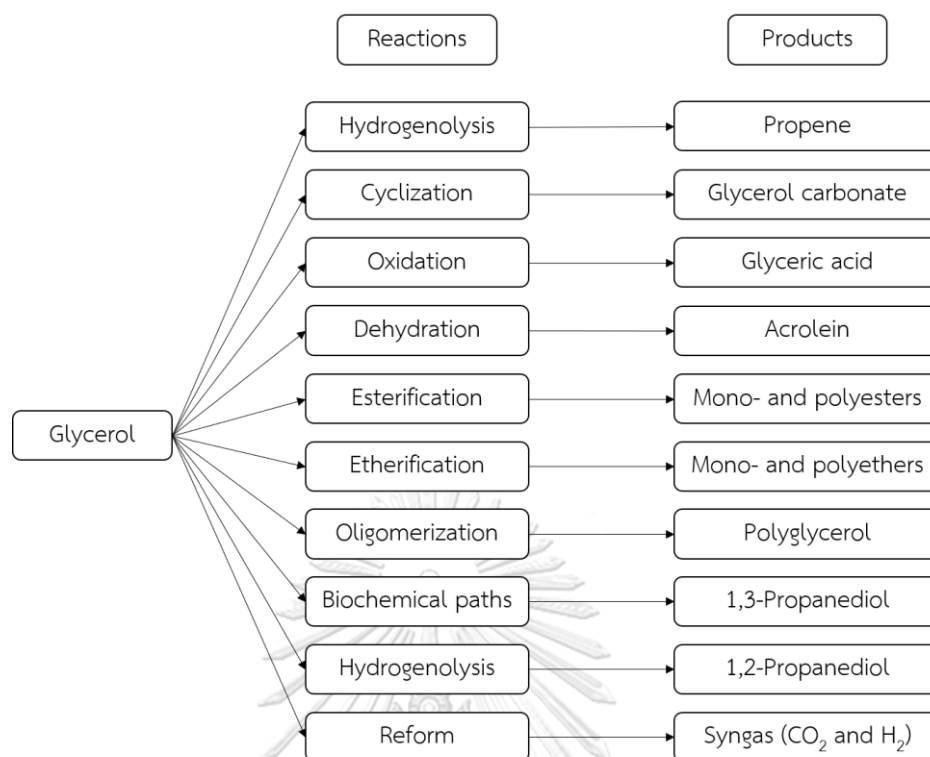
Figure 3 Pathway for possible glycerol derivatives[16]

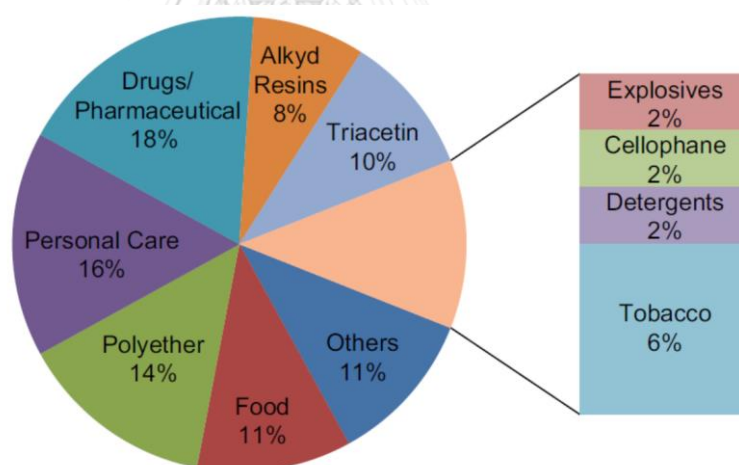In recent years, the interesting reaction for glycerol transformation to higher-value products is the hydrogenolysis of glycerol to propanediol. Wanted products from the hydrogenolysis of glycerol are 1,2-propanediol (1,2-PDO) and 1,3-propanediol (1,3-PDO). Among them, 1,3-PDO reveals a higher value than of 1,2-PDO. Thus, the hydrogenolysis of glycerol to 1,3-PDO is gained more attention.

2.2 Hydrogenolysis of glycerol to 1,3-propanediol

Because glycerol has more -OH group than the propanediol products, the hydrogenolysis of glycerol aims to remove -OH group together with one H atom addition. Moreover, another approach is adding H_2 molecule following H_2O discharge[17].

The hydrogenolysis is two steps reaction of bonds dissociation of chemical reactant following by hydrogen filling. The hydrogenolysis of C-C bond, as known as hydrocracking, which widely used in petroleum chemistry, is a reaction for shortening the carbon chain length, as shown in Eq. 1[18]. On the other hand, the hydrogenolysis

of C-O bond is a method to get rid of the content of oxygen in a substrate, particularly C-OH bond, which was extensively used to convert biomass to fuel or chemicals as shown in Eq. 2[19].
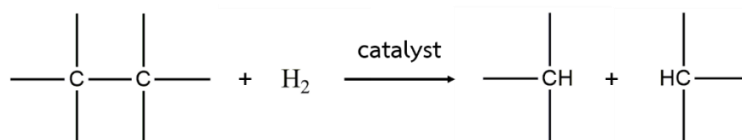
Eq. 1
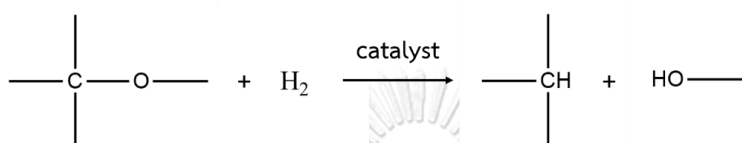
Eq. 2

The proposed mechanisms pathway of glycerol hydrogenolysis is illustrated in Figure 4. Firstly, C-O bond dissociation of glycerol hydrogenolysis is taken place to two products, including 1,2-PDO and 1,3-PDO. Then, the 1,2-PDO and 1,3-PDO can be over hydrogenolysis to 1-propanol (1-PrOH), 2-propanol (2-PrOH), and propane. Moreover, the products such as ethylene glycol, ethanol, methanol, ethane, and methane are produced from C-C hydrogenolysis of glycerol.
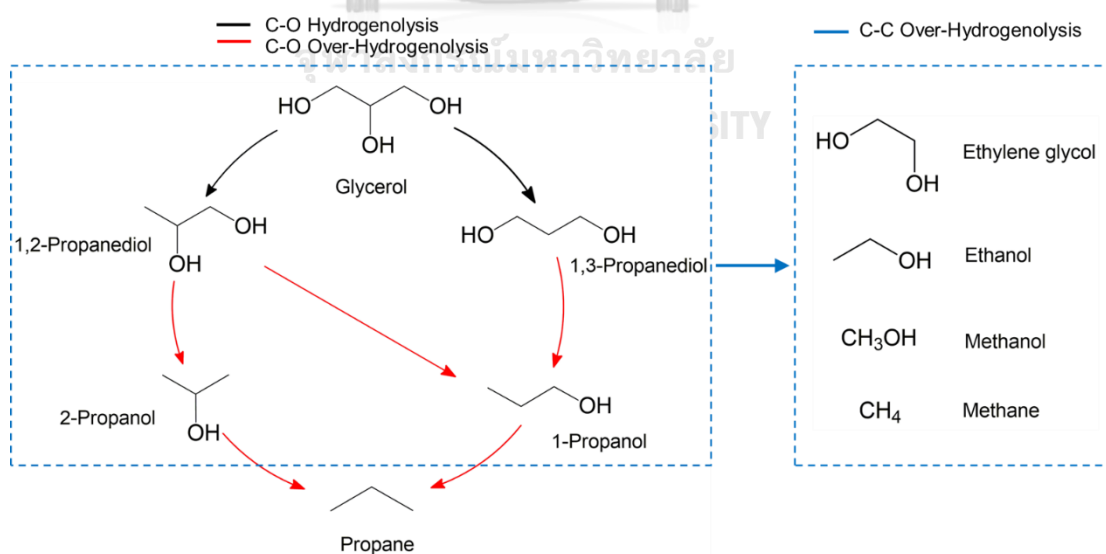
Figure 4 Products and byproducts from hydrogenolysis of glycerol

The many mechanisms of glycerol hydrogenolysis have been proposed, and the pathway that was operated depending on the system of reaction. Acidic, basic, or metal catalytic properties are parameters for a selective pathway. The mechanism of glycerol hydrogenolysis has three routes to achieve the propanediol (Figure 5), consist of dehydration-hydrogenation, dehydrogenation-dehydration-hydrogenation, and direct hydrogenolysis[20].
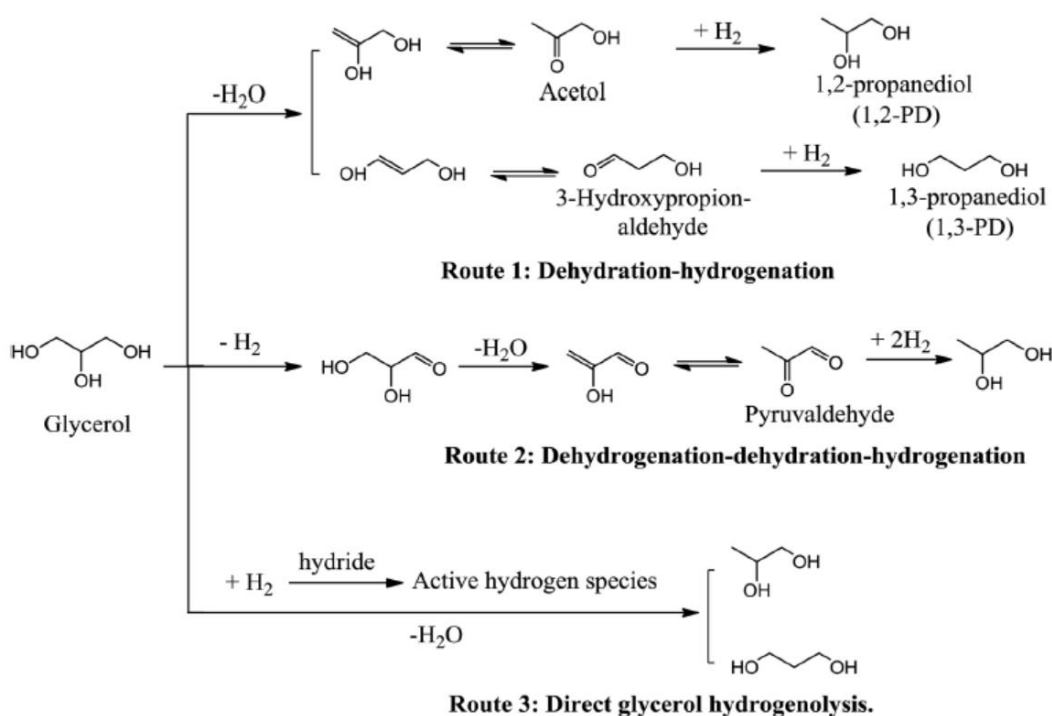
Figure 5 Mechanisms of glycerol hydrogenolysis to produce propanediol

In the dehydration-hydrogenation route, the acid catalyst is used for glycerol dehydration to form intermediate. After that, the intermediate is hydrogenated to be the product. The intermediates of dehydration and hydrogenation are acetol and 3-hydroxypropionaldehyde (3-HPA), respectively. Acetal is a dehydrated intermediate which is hydrogenated to 1,2-PDO through -OH group removal at the first position of glycerol (Figure 5, Route 1). On the contrary, 1,3-PDO is formed via hydrogenation of 3-HPA intermediate, which -OH group is dehydrated at the second position of glycerol, while the dehydrogenation-dehydration-hydrogenation (Figure 5, Route 2) is

a reaction that produced the mainly 1,2-PDO under neutral water and alkali condition.

## 2.3 Catalysts and literature reviews

The catalysts for hydrogenolysis of glycerol have two functions of catalytic to remove the -OH group and to fill the hydrogen. First, the function that using for -OH group removal is the acidic or basic function. Second, the oxidation-reduction process is used for hydrogen adding. The catalyst components for hydrogenolysis of glycerol include metal and metal oxides, or acidic, or basic supports. The metal component used for hydrogen activation and the support used to provide acid-base performance. The catalysts for hydrogenolysis of glycerol are divided into two groups, transition, and noble metal, based on the metal types.

In 1988 and 1991, Montassier et al.[21] studied propanediol production from hydrogenolysis of glycerol using Ru particles on charcoal (Ru/C) catalysts. As a result, the pathway of glycerol hydrogenolysis is dehydrogenation-dehydration-hydrogenation (Route 2, Figure 5). First, dehydrogenation of glycerol is generated over the metal surface, and glyceraldehyde, which is the intermediate chemical of the reaction, is produced. Second, 2-hydroxyacrolein and pyruvaldehyde are two intermediate chemicals derived from dehydration in the base condition. After that, all the intermediate chemicals are reacted through hydrogenation with high pressure H_2 gas. 1,2-PDO is a main product from the reaction. The selectivity of 1,2-PDO is higher than the selectivity of 1,3-PDO. And researchers found that the alkali condition increasing of the reaction causes the significant increase of reaction rate because the intermediate favors dehydration in the alkali condition. Lahr and Maris get similar results in 2003[22], 2005[23], and 2007[24], respectively.

In 2005, Dasari et al.[25] studied the hydrogenolysis of glycerol to propylene glycol using different metal-doped over carbon-based support. The results showed that the reduced Copper-chromite catalyst is identified as the most effective catalyst. The mild reaction conditions, 200 °C and 200 psi, provide high selectivity (85%) and good conversion (54.8%) more than other metal such as Ni/C, Ru/C, Pd/C, and Pt/C.

The researchers propose two steps of the reaction mechanism to convert glycerol to propylene glycol (Figure 6).
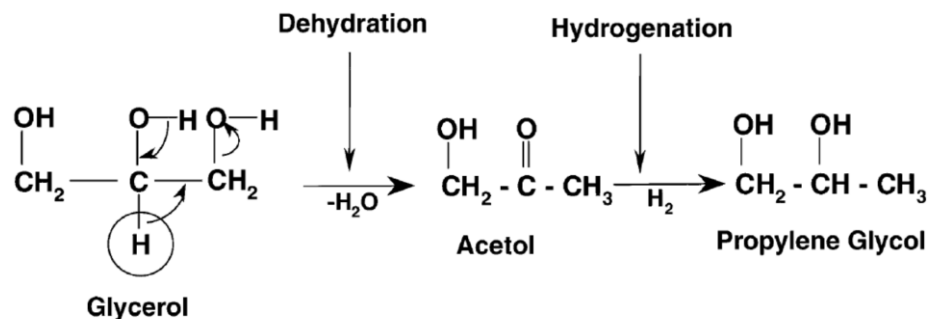

Figure 6 Proposed reaction mechanism for conversion of glycerol to propylene glycol

In 2007, Tomishige *et al.*[26] evaluated the catalytic performance of noble-metal supported on Al_2O_3 and SiO_2. As a result, Rh/SiO_2 is presented higher activity and selectivity at low temperature (120 $^\circ$C) than Ru/C. The highest conversion and 1,3-PDO selectivity of Rh/SiO_2 are 7.2% and 7.9%, respectively. The reaction route on Rh/SiO_2 is differenced from Ru/C via the products from hydrogenolysis of glycerol. Rh/SiO_2 catalyst promotes the propanol formation from 1,2-PDO, while Ru/C favors to proceed with the generation of propanol from 1,3-PDO.

In 2011, Tomishige *et al.*[27] discussed the mechanism of glycerol hydrogenolysis to 1,3-PDO over the Re-added noble metal catalyst. The standard condition of the reaction is following 120 $^\circ$C, 8 MPa initial pressure of H_2, and 12 h reaction time. The result showed that $Ir-ReO_x/SiO_2$ is selective to produce 1,3-PDO. Consequently, the mechanism of glycerol hydrogenolysis is a direct pathway to form 1,3-PDO via 2,3-dihydroxypropoxide. As shown in Figure 7, the transition state of glycerol adsorbed on Re species, firstly, the $-CH_2OH$ group of glycerol is adsorbed on the surface of ReO_x to form alkoxide. Next, for 1,3-PDO production, the secondary C-O bond of 2,3-dihydroxypropoxide, the intermediate, is attacked by activated -OH group on Ir metal as depicted in Figure 7 (a). On the other hand, the remaining C-O bond cleavage of the intermediate is taken place by activated -OH group on Ir metal

leading to the production of 1,2-PDO (Figure 7 (b)). As Chia *et al.*[28] the identical mechanism of glycerol hydrogenolysis over Rh-ReO$_x$/C catalyst is reported.
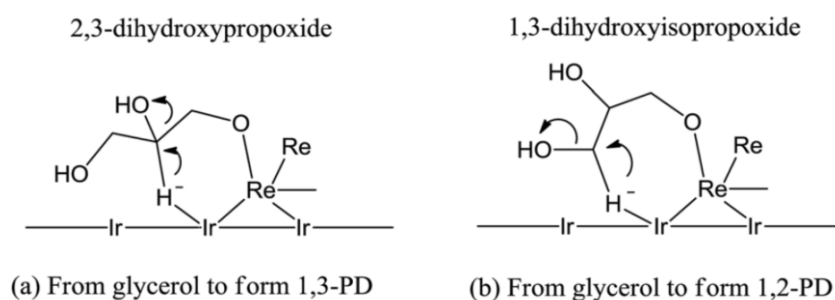
Figure 7 Model structures of the transition states of the hydride attack to the adsorbed substrate in the glycerol hydrogenolysis[27]

In 2012, Liu *et al.*[29] investigated the catalytic performance of mesoporous tungsten oxide (m-WO$_3$) supported Pt catalyst for hydrogenolysis of glycerol compared with commercial WO$_3$ under the reaction condition, 180 ^{o}C, 5.5 MPa H$_2$, 12 h and the mass ratio of catalyst/glycerol equal to 1:4. The evaporation-induced self-assembly method is used to synthesize the m-WO$_3$ using WCl$_6$ as a precursor. The results showed that Pt/m-WO$_3$ is more active and selective for hydrogenolysis of glycerol to produce a main product as 1,3-PDO than commercial cause the high dispersion of Pt and good reducibility of m-WO$_3$. As a result, the glycerol conversion reached 18%, and the selectivity of 1,3-PDO was 39.3%.

In 2015, Zhu *et al.*[30] studied the effect of various WO$_x$ contents over Pt/Al$_2$O$_3$ catalysts. The researchers found that 10 wt.% of WO$_x$ loading over Pt/Al$_2$O$_3$ catalyst gave approximately 50 times of 1,3-PDO yield (42.4%) compared with Pt/Al$_2$O$_3$ catalyst because of the existing of Brønsted acid sites. The Brønsted acid sites promote the secondary C-O bond cleavage of glycerol to produce 1,3-PDO, while Lewis acid sites favor to form 1,2-PDO via controlling the cleavage of primary C-O bond.

In 2015, Garcia *et al.*[31] studied the effect of bimetallic Pt/WO$_x$/Al$_2$O$_3$ catalysts to selective 1,3-PDO production from the hydrogenolysis of glycerol. The high

dispersion of polytungstate species over the catalyst surface led to the highest selectivity of 1,3-PDO due to Brønsted acidity is produced. The role of acidity and interaction between platinum and tungsten oxides are necessary for the selective hydrogenolysis of glycerol to 1,3-PDO. $Pt/WO_x/Al_2O_3$ catalysts were prepared by the sequential wetness impregnation method. The activity test results showed when the platinum content is increased from 1 wt.% to 9 wt.%, the conversion of glycerol and the selectivity of 1,3-PDO also increased from 25.6% to 60.3% and 16.4% to 31.2%, respectively.

In 2016, Garcia *et al*.[13] studied the effect of WO_x to be selective for the hydrogenolysis of glycerol over $Pt/WO_x/Al_2O_3$ catalysts. The catalytic reaction was tested under the reaction condition, 200 ^{o}C, 90 bar of H_2, and 4 h of reaction time, using the reduced catalysts. The 9Pt8WAl catalyst is reported as a high yield of 1,3-PDO of 38.5%. The researchers found the three roles of tungsten oxide in the hydrogenolysis of glycerol, as follows: (1) strong anchoring site for primary hydroxyl group of glycerol (2) protons provider (3) stabilizer of the secondary carbocation.

In 2017, Garcia *et al*.[32] doped bimetallic $Pt-WO_x$ on supports, aluminium oxide, and HZSM-5, to study structure-activity relationship for hydrogenolysis of glycerol. The results showed that the important parameters to produce 1,3-PDO are tungsten surface density and the closed contact between Pt and WO_x. The density of the tungsten surface controls the type of WO_x species generated on the surface of catalyst. Polytungstate produced the weak Brønsted acidity, which is necessary to selectively produce 1,3-PDO. For $Pt/WO_x/Al_2O_3$ catalyst, the increase of Pt dispersion promotes the high conversion of glycerol leading to 1,2-PDO and 1,3-PDO formation. However, the increment of Pt content on catalyst surface significantly enhance the amount of 1,3-PDO production. Moreover, the assistance of WO_x and Pt metal promoted the selectivity of intermediate carbocation to 1,3-PDO.

2.4 Sintering

Sintering is a process of metal aggregating to a larger size on the surface of catalyst during high temperature, which weakens the interaction between metal and support. Hence, the surface area of used catalyst is decreased leading to loosing of

catalytic performance comparing to the fresh catalyst. To prevent the metal sintering process, increment the interaction between metal and support on the catalyst surface is an effective solution to solve this problem[33].

Garcia et $al.$[32] studied the structure of Pt-WO$_x$ with 10 wt.% W content over Al-based supports using X-ray diffraction measurement. The result is showed that the diffraction peak of Pt metal on used 2Pt9W Al^{com} catalyst is shaper than the fresh catalyst at 2θ = 39.9°. They reported that the Pt metal on the Al-based support catalyst is sintered during the reaction at high temperature and pressure (200 $^{\circ}$C and 25 bar).

2.5 Fouling and Coking

Fouling is a physical deposition of components from the liquid phase onto catalyst surface. This process leads to activity losing of active sites due to blockage of sites and/or pores. Coking is one kind process of fouling that hydrocarbons decompose or condensate on catalyst surface[34]. These are deactivation types of catalyst which affected to decrease of catalytic activity.

Gandarias et $al.$[35] studied hydrogenolysis of glycerol under mild reaction conditions (493K and 45 bar of H$_2$ pressure) using Pt supported on amorphous silico alumina (Pt/ASA). They reported the addition of Pt metal could reduce the coke formation from 6.2% on ASA support to 5.4% on Pt/ASA catalyst because of Pt metal cleavage C-C bond.

CHAPTER III

EXPERIMENTAL

This chapter mentions the used chemicals in catalysts preparation including steps of preparing the catalysts via wet impregnation method. Next, the step by step of glycerol hydrogenolysis is referenced to imitate easily. Finally, the conditions of Gas-Chromatograph and measurements of catalysts characterization are shown in the chapter.

3.1 General of Chemicals

The list of chemicals for the hydrogenolysis of glycerol is shown in Table 1.

Table 1 Chemicals in the hydrogenolysis of glycerol

Chemicals	Formula	Supplier
Alumina (lab grade)	γ-Al$_2$O$_3$	Kemaus
Glycerol	C$_3$H$_8$O$_3$	Sigma-Aldrich
Ammonium(meta)tungstate hydrate	(NH$_4$)$_6$H$_2$W$_{12}$O$_{40}$ · xH$_2$O	Sigma-Aldrich
Chloroplatinic acid hydrate	H$_2$PtCl$_6$	Sigma-Aldrich

3.2 Catalyst Preparation

The Pt/WO$_x$/γ-Al$_2$O$_3$ catalyst was prepared using wet impregnation method. And the catalyst preparation processes are as follow.

3.2.1 Pt/γ-Al$_2$O$_3$

Pt/γ-Al$_2$O$_3$ catalyst was prepared by wet impregnation method. First, the powder of γ-Al$_2$O$_3$ (Kemaus) was calcined in static air at 900 °C for 3 h. After that, the chloroplatinic acid hydrate (H$_2$Cl$_6$Pt.nH$_2$O, Sigma-Aldrich, 38% Pt basis) was used as a precursor. Next, 5 wt.% of H$_2$Cl$_6$Pt were dissolved in deionized water to be a completed solution and impregnated on the γ-Al$_2$O$_3$ powder by stirring at 500 rpm for 16 h. Finally, the prepared catalysts were dried overnight at 110 °C and calcined

in airflow at 300 °C for 3 h. 5Pt/γ-Al$_2$O$_3$ catalyst where 5 is indicated 5 wt.% of Pt metal was used in the catalytic reaction.

3.2.2 WO$_x$/γ-Al$_2$O$_3$

WO$_x$/γ-Al$_2$O$_3$ catalyst was prepared via wet impregnation method. First, the calcined γ-Al$_2$O$_3$ powder from the previous step was impregnated with 10 wt.% of ammonium metatungstate (AMT, (NH$_4$)$_6$(H$_2$W$_{12}$O$_{40}$).nH$_2$O, Sigma-Aldrich, ≥99.99%) which dissolved in DI water as a solution. After that, the impregnated γ-Al$_2$O$_3$ was stirred at 500 rpm for 16 h. The WO$_x$/γ-Al$_2$O$_3$ was dried overnight at 110 °C. Finally, the catalyst was calcined in airflow at 900 °C for 3 h.

3.2.3 Pt/WO$_x$/γ-Al$_2$O$_3$

Pt/WO$_x$/γ-Al$_2$O$_3$ catalyst was prepared by wet impregnation method. First, WO$_x$/γ-Al$_2$O$_3$ catalyst from the previous step was impregnated with 5 wt.% of H$_2$Cl$_6$Pt as a precursor which is dissolved in DI water. Second, the impregnated catalyst was stirred at 500 rpm for 16 h. After the impregnation was finished, the catalyst was dried overnight at 110 °C and calcined in airflow at 300 °C for 3 h. 5Pt/WO$_x$/γ-Al$_2$O$_3$ catalyst where 5 is indicated 5 wt.% of Pt metal was used in the catalytic reaction.

3.3 Hydrogenolysis Reaction

The catalytic reaction of glycerol hydrogenolysis to 1,3-PDO was tested. First, 0.6 g of catalyst and 3 wt.% of aqueous glycerol solution were placed into 100 mL stainless steel autoclave, as showed in Figure 8. Second, the system was flushed three times with 5 bar of H$_2$ and pressurized with H$_2$ to reaction pressure of 5 bar. Then, the temperature of the system was heated to 140 °C and stirred at 800 rpm for 6 h. After the reaction was finished, the system was cooled down immediately to ambient temperature overnight to condense all components in gas to the liquid phase. Subsequently, 0.3 g of ethylene glycol was added as the internal standard. After that, the sample was centrifuged to separate solid catalysts from the liquid phase. And the solid catalysts were washed several times with DI water and dried at 110 °C until a weight becomes stable. Finally, the products of the liquid phase were analyzed using a Shimadzu 14B gas chromatograph with DB-WAX-UI capillary column

equipped with a flame ionization detector (30 m × 0.32 mm × 0.5 μm) as the GC condition as shown in Table 2. To determine the catalyst stability, the used catalysts were recycled to the second hydrogenolysis of glycerol as the same reaction condition. The conversion of glycerol and selectivity of each liquid product was calculated using the following equations, respectively.

$$\text{Conversion (\%)} = \frac{\text{moles of glycerol (in) - moles of glycerol (out)}}{\text{moles of glycerol (in)}} \times 100$$

$$\text{Selectivity (\%)} = \frac{\text{moles of product}}{\text{moles of glycerol (in) - moles of glycerol (out)}} \times 100$$

$$C_3 \text{ Moles Balance (\%)} = \frac{\Sigma \text{ moles of product + moles of glycerol (out)}}{\text{moles of glycerol (in)}} \times 100$$

Table 2 The analysis conditions of Gas Chromatograph

Gas Chromatograph	Shimadzu GC 14-B
Detector	FID
Column	DB-WAX-UI capillary column
Carrier Gas	Helium (99.99 vol. %)
Make-up Gas	Air (99.9 vol. %)
Column Temperature	60 $^\circ$C
Injector Temperature	250 $^\circ$C
Detector Temperature	250 $^\circ$C
Time Analysis (min)	30
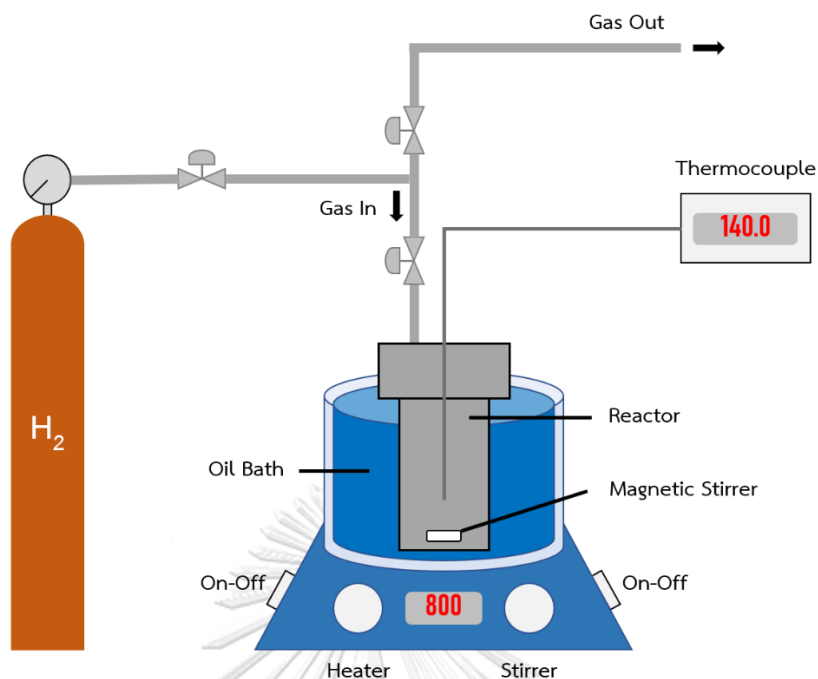
Figure 8 Experimental equipment for hydrogenolysis of glycerol

3.4 Catalysts Characterization

3.4.1 N_2 Physisorption

N_2 physisorption was used to observe the surface area of catalysts by a single point on the N_2 adsorption isotherm method using the Micromeritics Chemisorb 2750 Pulse Chemisorption system. 50 mg of the catalysts are pretreated at 300 °C for 1 h under N_2 flow. Then, the system temperature was reduced to -196 °C for 30% of N_2/He adsorption. Finally, the temperature of the catalysts system was heated up to room temperature for desorption. The specific surface area can be calculated by dividing the peak area with the weight of catalyst sample.

3.4.2 Inductively Coupled Plasma (ICP)

The amounts of Pt and W metal leaching from the surface of catalysts into liquid phase are determined by inductively coupled plasma optical emission spectrometer (ICP-OES) on a 2100 DV from Perkin Elmer. After the separation of solid catalyst, 1 mL of the solution is dissolved with DI water. The energy from coupled plasma is used in the measurement.

3.4.3 Scan Electron Microscope (SEM)

The chemical composition attributed to the surface of the catalysts is examined with SEM-EDX using Link Isis series 300 program SEM (JEOL model JSM-5800LV).

3.4.4 X-ray Diffraction (XRD)

Powder X-ray diffraction (XRD) measurement is used to characterize the patterns of catalysts. The diffraction patterns are collected by Bruker D8 Advance using Cu Kα irradiation at 2θ = 20° to 80° with a 0.05° s^{-1} step size.

3.4.5 IR Spectra of Pyridine Adsorption (Py-IR)

Types of acid sites of catalysts are analyzed from the FTIR spectra of adsorbed pyridine via a Bruker Equinox 55 FT-IR spectrometer equipped with mercury cadmium telluride (MTCB) detector. The 55 mg of samples is pretreated under vacuum at 300 °C for 1 h with a ramping rate 10 °C/min. After that, the system is cool down to 50 °C to adsorbed pyridine and collected IR spectra at the same temperature.

3.4.6 Temperature-Programmed Oxidation (TPO)

To analyze the amount of carbon contents in the catalyst, temperature-programmed oxidation (TPO) was used to measure weight changing on the material, which was lost during reaction testing. Moreover, the catalyst was determined the chemical phenomena such as the temperature of catalyst decomposition and oxidation reaction between gas and solid. 10-20 mg of the specimen was used to operate the temperature program at 25 to 1000 °C with 10 °C/min of temperature ramping using N$_2$ UHP as the carrier gas.

3.4.7 Fourier-transform Infrared Spectroscopy (FTIR)

To determine chemical structure on the catalyst surface, Fourier-transform infrared spectroscopy (FTIR) was used to analyze the functional group of the catalyst using Nicolet 6700 FTIR spectrometer. 50-100 mg of catalyst were pressed to powder disk. After that, the wavenumbers of the infrared spectrum were recorded at 4000-400 cm^{-1}.

CHAPTER IV

RESULTS AND DISCUSSION

This chapter mentions the several studies and results containing the effect of a reusable catalyst on catalytic activity, the influence of tungstate oxide addition, and the effect of platinum loading on the sintering of catalyst during the glycerol hydrogenolysis to 1,3-PDO. The characterizations of catalyst specimens were investigated using the technique such as N_2-physisorption, ICP, SEM-EDX, XRD, Py-IR, TPO, and FTIR.

4.1 Catalyst Properties

4.1.1 N_2 Physisorption

The physical property of fresh catalysts is shown in Table 3. The surface area of catalyst specimens is decreased with the addition of WO_x and Pt metal on catalyst comparing bared γ-Al_2O_3 support. Diminish of the surface area of impregnated catalysts such as WO_x/γ-Al_2O_3 and Pt/γ-Al_2O_3 may be caused by hindrance or blockage the pores of the support. As a result, the introduction of Pt metal on WO_x/γ-Al_2O_3 catalyst also reduces the surface area described through the same assumption[31, 36].

Table 3 N_2 physisorption and acidity of fresh catalyst

Catalyst	Surface area (m²/g) [a]	B/L acid ratio [b]
γ-Al_2O_3	90	N.A.
WO_x/γ-Al_2O_3	38	N.A.
5Pt/γ-Al_2O_3 (fresh)	48	0.17
5Pt/WO_x/γ-Al_2O_3 (fresh)	33	0.26

[a] surface area based on gram of catalyst

[b] ratio of Brønsted and Lewis acid sites from FTIR of pyridine adsorption

N.A. = non-analysis

4.1.2 IR Spectra of Pyridine Adsorption (Py-IR)

To classify acidity difference and evaluate type of acid sites (Brønsted and Lewis sites) of 5Pt/γ-Al$_2$O$_3$ and 5Pt/WO$_x$/γ-Al$_2$O$_3$ catalysts, FTIR combining to specific pyridine adsorption analysis is performed. The FTIR spectrum of pyridine adsorption on fresh 5Pt/γ-Al$_2$O$_3$ and 5Pt/WO$_x$/γ-Al$_2$O$_3$ catalysts are revealed in Figure 9.

Recently, there are several researches reporting that appearance of characteristic peak in a range of 1450 cm^{-1} and 1614 cm^{-1} evidence Lewis acid sites (L)[30, 37] whereas the occurrence of characteristic peak around 1540 cm^{-1} and 1640 cm^{-1} illustrates the characteristic peaks of Brønsted acid site (B)[38]. Moreover, observation of characteristic peak, particularly at 1490 cm^{-1}, reveals the mixture of Brønsted and Lewis sites (B+L) of catalysts[39].

The 5Pt/γ-Al$_2$O$_3$ and 5Pt/WO$_x$/γ-Al$_2$O$_3$ catalysts exhibit both of Brønsted and Lewis acid site that the signal of Lewis acid site shows higher intensity than Brønsted acid site. These results indicate Lewis acid sites on 5Pt/γ-Al$_2$O$_3$ and 5Pt/WO$_x$/γ-Al$_2$O$_3$ catalysts are dominant.
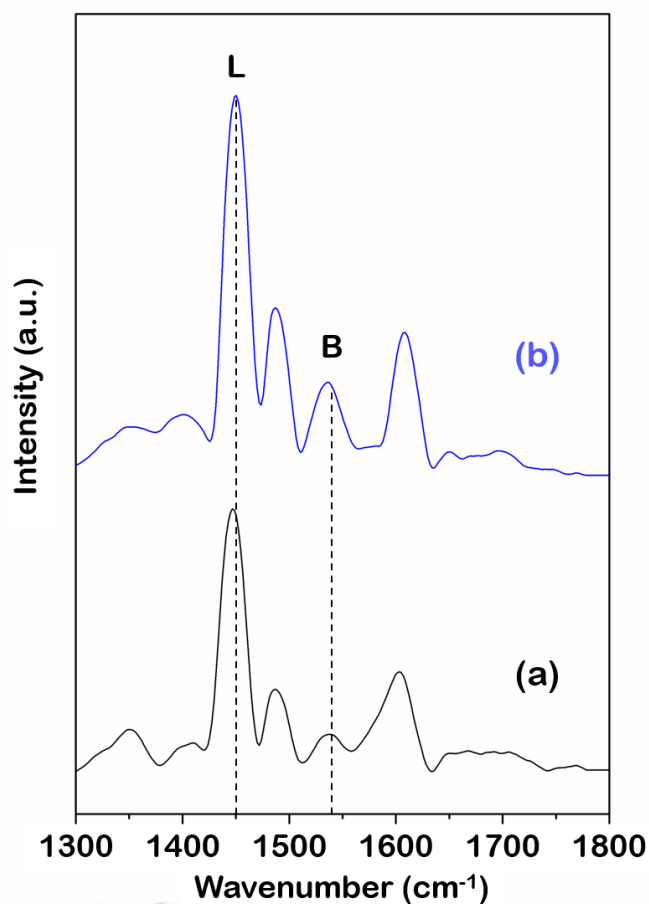
Figure 9 Pyridine adsorption of fresh 5Pt/γ-Al$_2$O$_3$ (a) and 5Pt/WO$_x$/γ-Al$_2$O$_3$ (b) catalysts

4.2 Catalytic Activity

Table 4 shows catalytic activity of fresh 5Pt/γ-Al$_2$O$_3$ and 5Pt/WOx/γ-Al$_2$O$_3$ catalysts in the hydrogenolysis of glycerol to 1,3-PDO using mild reaction condition: 140 °C, 5 bar of initial H$_2$ pressure and 6 h of reaction time. The results indicate glycerol conversion of 5Pt/γ-Al$_2$O$_3$ catalyst is 23.2%, while glycerol conversion of 5Pt/WO$_x$/γ-Al$_2$O$_3$ catalyst is 35.8%. The selectivity of wanted 1,3-PDO is 6.9% on 5Pt/γ-Al$_2$O$_3$ catalyst. However, 1,3-PDO selectivity on 5Pt/WO$_x$/γ-Al$_2$O$_3$ catalyst is 29%. Whereas, the selectivity of 1,2-PDO as a by-product in this study on 5Pt/γ-Al$_2$O$_3$ catalyst is decreased from 18.7% to 10.2% when WO$_x$ is doped on Pt-based catalyst.

These can suggest that $5Pt/\gamma$-Al_2O_3 catalyst is selective to 1,2-PDO, while $5Pt/WO_x/\gamma$-Al_2O_3 catalyst is selective to 1,3-PDO production.

From this result, the introduction of WO_x on Pt-based catalyst can improve the selectivity of wanted 1,3-PDO because the acidic property on catalyst is increased with the addition of WO_x content. As showed in Table 3, the acidic ratio of Brønsted and Lewis sites on $5Pt/\gamma$-Al_2O_3 catalyst is 0.17, while B/L ratio of $5Pt/WO_x/\gamma$-Al_2O_3 catalyst is 0.26.

Table 4 Conversion of glycerol and selectivity of each product in hydrogenolysis of glycerol under reaction conditions: 140 $^{\circ}$C, 5 bar of initial H_2 pressure and 6 h of reaction time

Catalyst	Conversion of glycerol (%)	Product selectivity (%)				C_3 Moles balance (%)
		1,3-PDO	1,2-PDO	1-PrOH	2-PrOH	
$5Pt/\gamma$-Al_2O_3 (fresh)	23.2	6.9	18.7	7.0	31.6	91.7
$5Pt/\gamma$-Al_2O_3 (used)	12.7	4.6	32.7	10.7	25.4	96.6
$5Pt/WO_x/\gamma$-Al_2O_3 (fresh)	35.8	29.0	10.2	11.6	21.1	89.9
$5Pt/WO_x/\gamma$-Al_2O_3 (used)	30.0	22.8	11.6	8.6	13.1	86.8

To study the stability of the catalyst, the several cycles of catalyst in hydrogenolysis of glycerol are investigated using the weight of catalyst in the second hydrogenolysis reaction, including reaction condition as same as the first time. The results of used catalyst in Table 4 show conversion of glycerol is decreased on both used catalysts; however, conversion of glycerol on $5Pt/WO_x/\gamma$-Al_2O_3 catalyst is slightly dropped from 35.8% to 30% while conversion of glycerol on $5Pt/\gamma$-Al_2O_3 catalyst is decreased from 23.2% to 12.7%. Moreover, the decrease of glycerol conversion on $5Pt/\gamma$-Al_2O_3 catalyst is larger than $5Pt/WO_x/\gamma$-Al_2O_3 catalyst (45.3% and 16.2%, respectively). In addition, the selectivity of 1,3-PDO on used $5Pt/\gamma$-Al_2O_3 catalyst is larger dropped than $5Pt/WO_x/\gamma$-Al_2O_3 catalyst (33.3% and 21.4%, respectively).

4.3 Catalyst Deactivations

    4.3.1 Chemical Analysis (ICP)

Leaching of Pt and W metals from $5Pt/\gamma\text{-}Al_2O_3$ and $5Pt/WO_x/\gamma\text{-}Al_2O_3$ catalysts during the hydrogenolysis of glycerol can be observed using ICP-OES measurement which the results of each Pt and W leaching, as well as the conversion of glycerol on each fresh and used catalysts, are concluded in Table 5.

For $5Pt/\gamma\text{-}Al_2O_3$ catalyst, the fresh $5Pt/\gamma\text{-}Al_2O_3$ catalyst provides 23.2% of glycerol conversion and 22×10^{-4} mg of Pt leaching after the hydrogenolysis process was complete. In case of used $5Pt/\gamma\text{-}Al_2O_3$ catalyst, conversion of glycerol is reduced to 12.7% while leaching of Pt element was also decreased to 6.6×10^{-4} mg. These results suggest that catalytic activity of used $5Pt/\gamma\text{-}Al_2O_3$ catalyst is obviously lower than that of fresh $5Pt/\gamma\text{-}Al_2O_3$ catalyst due to losing the active site by Pt leaching during the hydrogenolysis process.

For $5Pt/WO_x/\gamma\text{-}Al_2O_3$ catalyst, the fresh $5Pt/WO_x/\gamma\text{-}Al_2O_3$ catalyst shows 35.8% of glycerol conversion while leaching of Pt from $5Pt/WO_x/\gamma\text{-}Al_2O_3$ surface is detected as 0.5×10^{-4} mg after the first hydrogenolysis process while leaching of W element is observed as 182×10^{-4} mg. For used $5Pt/WO_x/\gamma\text{-}Al_2O_3$ catalyst, conversion of glycerol is detected as 30.0% without Pt leaching during the second hydrogenolysis process, whereas 51×10^{-4} mg of WO_x leaching was found.

As the results, catalytic activity measured by conversion of glycerol relates to the amount of Pt on catalyst surface implying that the impregnated Pt metal is a real active site for this hydrogenolysis reaction. Leaching of Pt element affects losing crucial active site leading to a significant decrement of catalytic activity, which is mentioned in case of employment of used $5Pt/\gamma\text{-}Al_2O_3$ and $5Pt/WO_x/\gamma\text{-}Al_2O_3$ catalyst for the second hydrogenolysis process. Hence, the introduction of WO_x to $\gamma\text{-}Al_2O_3$ before impregnating Pt active site to $WO_x/\gamma\text{-}Al_2O_3$ surface can improve catalytic activity by preventing Pt leaching from $5Pt/WO_x/\gamma\text{-}Al_2O_3$ to the liquid phase during hydrogenolysis reaction leading to few quantities of Pt metal in the liquid phase resulting higher catalytic activity comparing to $5Pt/\gamma\text{-}Al_2O_3$ catalyst.

Table 5 The amounts of Pt and W metal leaching from the surface of catalysts in the reaction solution based on the catalyst used

Catalyst	Catalytic cycle	Glycerol conversion (%)	Metal leaching [a] ($\times 10^{-4}$ mg)	
			Pt	W
5Pt/γ-Al$_2$O$_3$	Fresh	23.2	22.0	N.A.
	Used	12.7	6.6[a]	N.A.
5Pt/WO$_x$/γ-Al$_2$O$_3$	Fresh	35.8	0.5	182
	Used	30.0	0.0[a]	51[a]

[a] Metal leaching of used catalysts was calculated from based-on remained metals on catalysts after the first hydrogenolysis process.

N.A. = non-analysis

4.3.2 Scanning Electron Microscopy (SEM)

The morphological properties of 5Pt/γ-Al$_2$O$_3$ and 5Pt/WO$_x$/γ-Al$_2$O$_3$ in terms of fresh and used catalysts are analyzed using SEM-EDX technique which the SEM-EDX images of 5Pt/γ-Al$_2$O$_3$ and 5Pt/WO$_x$/γ-Al$_2$O$_3$ are showed in Figure 10.

For 5Pt/γ-Al$_2$O$_3$ catalyst, the perfect crystal of 5Pt/γ-Al$_2$O$_3$ powder without any dropped of Pt indicates a well dispersion of Pt on γ-Al$_2$O$_3$ in microscopic scale in both fresh and used cases as provided in Figure 10 (a and b). However, the detection of strong intensity of EDX image of Pt atom after the first hydrogenolysis process, as shown in Figure 10 (e and f) may imply growing of Pt active site, which evidences diffusion of Pt during the first hydrogenolysis reaction is carried. Diffusion of dispersed Pt to form larger Pt cluster exhibits aggregation behavior of Pt active site in the second hydrogenolysis reaction of glycerol.

For 5Pt/WO$_x$/γ-Al$_2$O$_3$ catalyst, good compatibility of Pt, WO$_x$, and γ-Al$_2$O$_3$ components also observed as a homogeneous pallet of 5Pt/WO$_x$/γ-Al$_2$O$_3$ which illustrated in Figure 10 (c and d). However, diffusion of dispersed Pt to larger Pt cluster given in EDX images as depicted in Figure 10 (g and h) may suggest that Pt metal can be moved on the surface to aggregate during hydrogenolysis of glycerol.
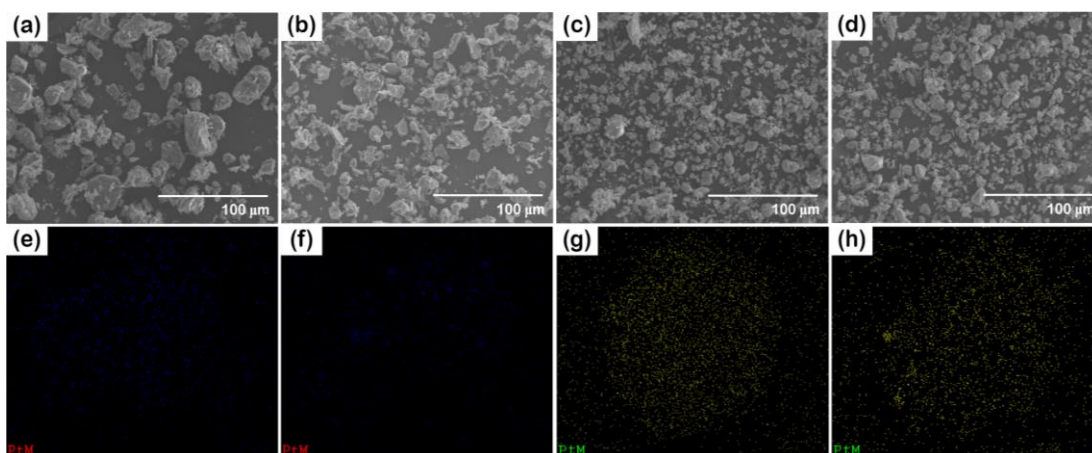
Figure 10 SEM images of (a) fresh, and (b) used 5Pt/γ-Al$_2$O$_3$ catalysts, as well as (c) fresh, and (d), used 5Pt/WO$_x$/γ-Al$_2$O$_3$ catalysts corresponding to SEM-EDX images of (e) fresh, and (f) used 5Pt/γ-Al$_2$O$_3$ catalysts, as well as (g) fresh, and (h) used 5Pt/WO$_x$/γ-Al$_2$O$_3$ catalysts

### 4.3.3 X-ray Diffraction Analysis (XRD)

The diffraction patterns of fresh and used catalysts for hydrogenolysis of glycerol are exhibited in Figure 11. It is well known that the characteristic diffraction peaks of clean γ-Al$_2$O$_3$ supporter have been reported at 2θ = 37.5°, 45.4° and 67.0° [40] whereas special characteristic diffraction peaks of pristine Pt metal have been illustrated at 2θ = 39.9° and 46.4°[32]. Moreover, the monoclinic WO$_3$ (m-WO$_3$) appears the unique diffraction peaks at 2θ = 23.6° and 33.5°[30]. However, the characteristic diffraction peaks of Pt metal and WO$_x$ species over γ-Al$_2$O$_3$ and WO$_x$/γ-Al$_2$O$_3$ surface were not clearly observed in this study because of well dispersion of the Pt and WO$_x$ particles on Al$_2$O$_3$ support reported by Zhu *et al.* and Feng *et al.*[30, 41].

For 5Pt/γ-Al$_2$O$_3$ catalyst, the combined XRD diffraction peaks of Pt and γ-Al$_2$O$_3$ supporter on fresh 5Pt/γ-Al$_2$O$_3$, which is demonstrated in Figure 11 (c), are not obviously detected via this XRD technique due to two main reasons. One is well dispersion of Pt metal on the γ-Al$_2$O$_3$ surface[41]; another is a very low amount of Pt metal on the γ-Al$_2$O$_3$ surface that the characteristic peaks of γ-Al$_2$O$_3$ are more dominant[39]. However, the characteristic diffraction pattern of used 5Pt/γ-Al$_2$O$_3$ is

changed after achievement first hydrogenolysis reaction indicates the surface transformation of used $5Pt/\gamma\text{-}Al_2O_3$ catalyst as depicted in Figure 11 (c_1).

Focusing on the characteristic diffraction peak of Pt metal at $2\theta = 39.9°$, the obvious shaper diffraction peak of Pt metal on used $5Pt/\gamma\text{-}Al_2O_3$ catalyst than that of fresh $5Pt/\gamma\text{-}Al_2O_3$ catalyst implies the occurrence of Pt sintering on $5Pt/\gamma\text{-}Al_2O_3$ catalyst during hydrogenolysis of glycerol[32] suffering decreasing of catalytic efficiency for glycerol conversion[42].

For $5Pt/WO_x/\gamma\text{-}Al_2O_3$ catalyst, the dominance diffraction pattern of $\gamma\text{-}Al_2O_3$ without emerging of other unique XRD diffraction peaks of Pt and WO_x is also suggested there are very small amount of Pt and WO_x species on the $\gamma\text{-}Al_2O_3$ surface corresponding to good dispersion of as exhibited in Figure 11 (d and d_1). Similar to $5Pt/\gamma\text{-}Al_2O_3$ catalyst, the appearance of shaper characteristic diffraction peak of Pt at $2\theta = 39.9°$ after the first hydrogenolysis of glycerol demonstrates the occurrence of Pt sintering during the hydrogenolysis process.
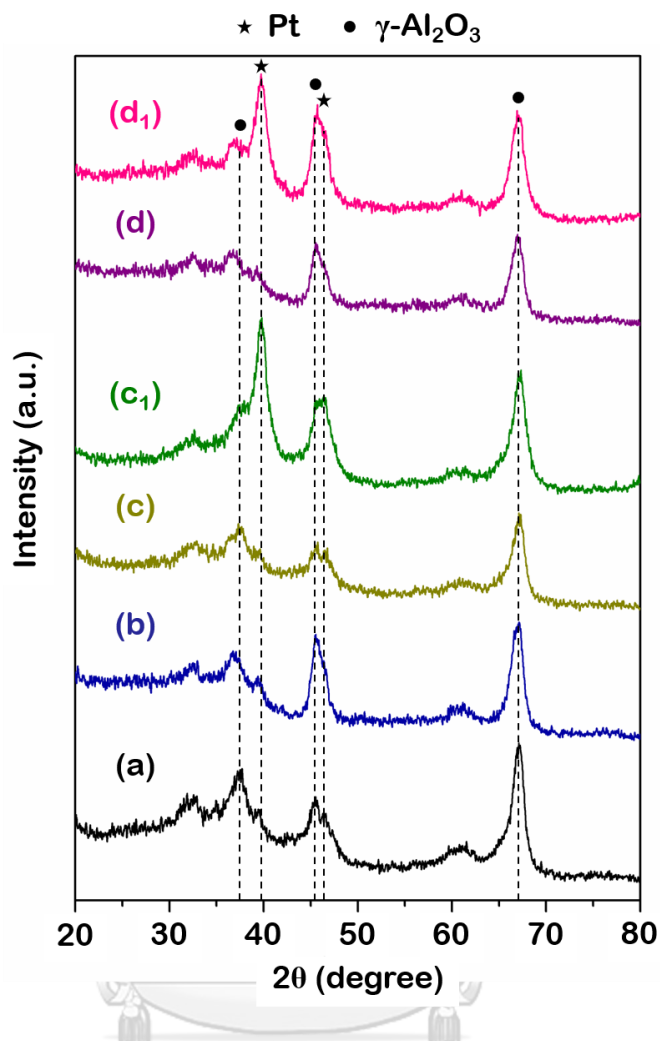
Figure 11 XRD diffraction patterns of (a) γ-Al_2O_3, (b) WO_x/γ-Al_2O_3, (c and c_1) 5Pt/γ-Al_2O_3, and (d and d_1) 5Pt/WO_x/γ-Al_2O_3 which the subscripts demonstrate the diffraction patterns of used catalysts

The Pt crystallites size from XRD data can calculate using Scherrer's Equation as follow:

$$D = \frac{K\lambda}{\beta \cos\theta}$$

Where D is crystallites size (nm), K is Scherrer constant using 0.9, λ is X-ray wavelength (0.15406 nm), β is full width at half maximum (FWHM, radians) and θ is a position of peak (radians).

The Pt metal sizes of Pt-based catalysts calculated from XRD results show in Table 6. For 5Pt/γ-Al$_2$O$_3$ catalyst, Pt metal sintering is detected after the hydrogenolysis of glycerol is completed. The size of Pt metal on the used catalyst is increased from 0.12 to 0.21 nm, comparing fresh catalyst. Similarly, the size of Pt metal on used 5Pt/WO$_x$/γ-Al$_2$O$_3$ catalyst is larger than fresh catalyst (0.18 and 0.10 nm, respectively). These results can suggest that the sintering of Pt metal occurs on both spent 5Pt/γ-Al$_2$O$_3$ and 5Pt/WO$_x$/γ-Al$_2$O$_3$ catalysts during the first reaction of glycerol hydrogenolysis under reaction condition.

Table 6 Size of Pt metal during hydrogenolysis of glycerol

Catalyst	Pt metal size [a] (nm)
5Pt/γ-Al$_2$O$_3$ (fresh)	0.12
5Pt/γ-Al$_2$O$_3$ (used)	0.21
5Pt/WO$_x$/γ-Al$_2$O$_3$ (fresh)	0.10
5Pt/WO$_x$/γ-Al$_2$O$_3$ (used)	0.18

[a] Calculated using Scherrer Equation

4.3.4 IR Spectra of Pyridine Adsorption (Py-IR)

For fresh 5Pt/γ-Al$_2$O$_3$ catalyst, a large difference of L and B signals illustrates low selectivity of 1,3-PDO using 5Pt/γ-Al$_2$O$_3$, as shown in Figure 9. Moreover, the diminishing of B signal in used 5Pt/γ-Al$_2$O$_3$, as depicted in Figure 12, reveals leaching of Pt species during the first hydrogenolysis reaction loses the crucial Brønsted acid site which is indispensable for 1,3-PDO production[30, 32, 43-44]. Hence, the selectivity of 1,3-PDO via used 5Pt/γ-Al$_2$O$_3$ is significantly decreased, as concluded in Table 4.

For fresh 5Pt/WO$_x$/γ-Al$_2$O$_3$ catalyst, the existence of WO$_x$ on 5Pt/WO$_x$/γ-Al$_2$O$_3$ catalyst enhances the signal of both Lewis and Brønsted acid sites comparing to 5Pt/γ-Al$_2$O$_3$ which the modified L and B signals can be observed at 1450 cm^{-1} and 1540 cm^{-1}, respectively. Although the addition of WO$_x$ can induce the Lewis acid site that is selective for the production of unwanted 1,2-PDO[30], an extremely increment of Brønsted acid site enlarges selectivity of 1,3-PDO. Therefore, the selectivity of 1,3-

PDO production is obviously enlarged via 5Pt/WO$_x$/γ-Al$_2$O$_3$ catalyst. Moreover, leaching of WO$_x$ during the first hydrogenolysis reaction, which is aforementioned in Table 5, slightly damages the Brønsted acid site of 5Pt/WO$_x$/γ-Al$_2$O$_3$ catalyst because the remained WO$_x$ component can keep Brønsted acidity of used 5Pt/WO$_x$/γ-Al$_2$O$_3$ catalyst. As a result, the selectivity of 1,3-PDO applying by used 5Pt/WO$_x$/γ-Al$_2$O$_3$ catalyst is still high as 22.8%, as provided in Table 4.

Consequently, 1,3-PDO can be produced on both 5Pt/γ-Al$_2$O$_3$ and 5Pt/WO$_x$/γ-Al$_2$O$_3$ catalysts that the existence of Pt species affects only activity of glycerol conversion while doping of WO$_x$ species determines the selectivity of 1,3-PDO production. These results are confirmed by previous reliable investigations[30, 45]. For reusing of catalyst to the second hydrogenolysis cycle as showed results of acid ratio in Table 7, leaching of Pt metal from fresh 5Pt/γ-Al$_2$O$_3$ during previous hydrogenolysis process diminish the active site which is essential for the conversion of glycerol reactant while the tiny Brønsted acidity of 5Pt/γ-Al$_2$O$_3$ is also vanished (B/L = 0.09) resulting extremely diminution of selectivity of 1,3-PDO production. In the case of used 5Pt/WO$_x$/γ-Al$_2$O$_3$ catalyst, leaching of WO$_x$ during slightly reduces Brønsted acidity of 5Pt/γ-Al$_2$O$_3$ (B/L = 0.22) resulting in overall selectivity of 1,3-PDO production slightly drops. Moreover, leaching of WO$_x$ also declines steric hindrance resulting accumulation of Pt site. Therefore, the activity of glycerol conversion on used 5Pt/WO$_x$/γ-Al$_2$O$_3$ is also significantly reduced.
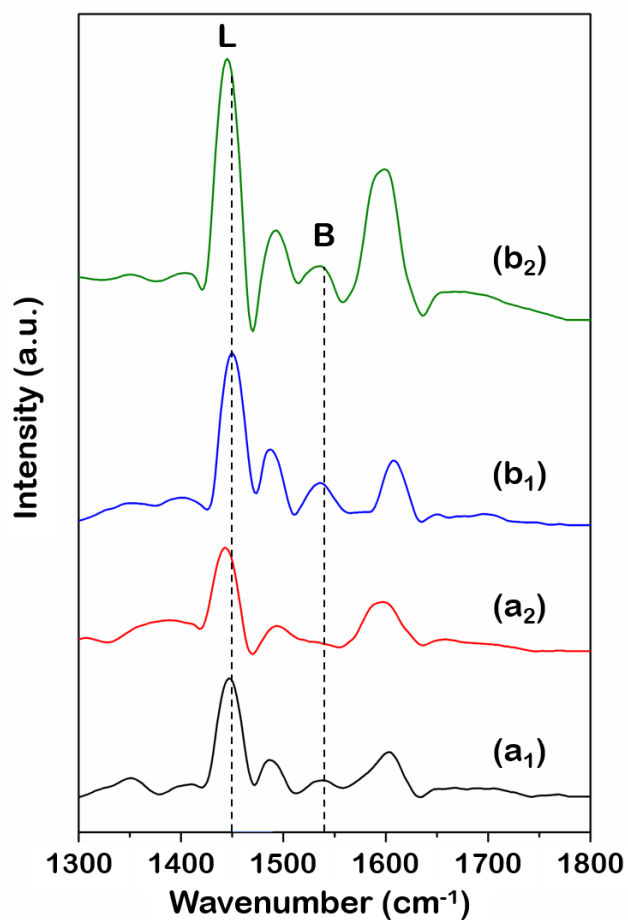
Figure 12 FTIR of adsorbed pyridine of fresh (a$_1$) and used (a$_2$) on 5Pt/γ-Al$_2$O$_3$ including fresh (b$_1$) and used (b$_2$) 5Pt/WO$_x$/γ-Al$_2$O$_3$ catalysts

Table 7 The acidity concentration of the catalysts measured by Py-IR

Catalyst	Glycerol conversion (%)	Selectivity (%)		Acid sites (a.u./g$_{cat}$)		B/L ratio[a]
		1,3-PDO	1,2-PDO	Brønsted	Lewis	
5Pt/γ-Al$_2$O$_3$ (fresh)	23.2	6.9	18.7	0.23	1.41	0.17
5Pt/γ-Al$_2$O$_3$ (used)	12.7	4.6	32.7	0.11	1.18	0.09
5Pt/WO$_x$/γ-Al$_2$O$_3$ (fresh)	35.8	29.0	10.2	0.52	2.02	0.26
5Pt/WO$_x$/γ-Al$_2$O$_3$ (used)	30.0	22.8	11.6	0.76	3.40	0.22

[a] A concentration proportional of Brønsted and Lewis acid sites

4.3.5 Temperature-Programmed Oxidation (TPO)

The temperature of coke removal and the amount of coke formation on used catalysts in hydrogenolysis of glycerol is determined by TPO. Figure 13 shows the TPO curves of used $5Pt/\gamma$-Al_2O_3 and $5Pt/WO_x/\gamma$-Al_2O_3 catalyst. The results give three peaks of catalyst weight changing: 30-150, 150-400, and 400-600 °C, respectively. The first peak is moisture and physical absorbents discharging, the second narrow peak can be attributed to the soft coke (high H/C ratio), and the sharp peak between 400-600 °C is reported as hard coke (low H/C ratio)[34, 46]. The peak of soft coke represents the coke formation on the metal surface of the catalyst, and the peak of hard coke indicates the coke formation on the surface of support[47]. From the results, coke formation on used $5Pt/\gamma$-Al_2O_3 catalyst is occurred on both surfaces of metal and support. But used $5Pt/WO_x/\gamma$-Al_2O_3 catalyst has the only deposition of coke formation on the support surface.
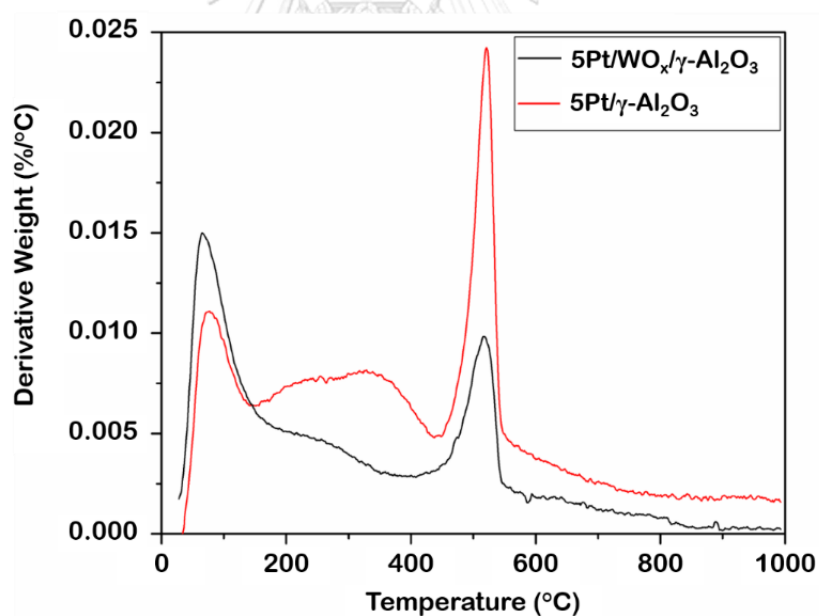
Figure 13 TPO curves of used $5Pt/\gamma$-Al_2O_3 and $5Pt/WO_x/\gamma$-Al_2O_3 catalysts

As the TPO results, weight transformation is detected on both used $5Pt/\gamma$-Al_2O_3 and $5Pt/WO_x/\gamma$-Al_2O_3 catalysts. Higher derivative weight can be suggested that higher carbon content, which is discharged from catalyst surface at high temperature,

is formed on catalyst[46]. Table 8 shows the amount of weight loss on used 5Pt/γ-Al$_2$O$_3$ and 5Pt/WO$_x$/γ-Al$_2$O$_3$ catalysts based on the initial weight of the sample. The amount of coke formation in terms of weight changing on 5Pt/γ-Al$_2$O$_3$ catalyst is 3.3%, which higher than 1.7% in 5Pt/WO$_x$/γ-Al$_2$O$_3$ catalysts.

Table 8 Amount of weight loss on used 5Pt/γ-Al$_2$O$_3$ and 5Pt/WO$_x$/γ-Al$_2$O$_3$ catalysts

Catalyst	Weight loss (%) [a]
5Pt/γ-Al$_2$O$_3$	3.3
5Pt/WO$_x$/γ-Al$_2$O$_3$	1.7

[a] Base on weight changing of catalyst at a temperature of soft and hard coke formation

4.3.6 Fourier-transform Infrared Spectroscopy (FTIR)

FTIR technique is used to determined functional groups on catalyst surface; especially, polymeric coke formation. To confirm types of functional groups on the catalyst surface, Figure 14 shows the FTIR spectra of used 5Pt/γ-Al$_2$O$_3$ and 5Pt/WO$_x$/γ-Al$_2$O$_3$ catalysts at wavenumber 1800-1400 cm^{-1}. At wavenumber range 1700-1600 cm^{-1} implies C=C bond stretching[48]. The small peak at 1630 cm^{-1} indicates the vibration of the C=C bond in the aromatic ring represents hard coke formation[46]. This result is good agreement with adsorption of aromatic coke on the metal surface of used 5Pt/γ-Al$_2$O$_3$ catalyst, which is detected by the TPO technique[49-50]. As TPO and FTIR results, this can be suggested that coke formation affects to glycerol conversion in hydrogenolysis reaction[51] as reported in Table 4.
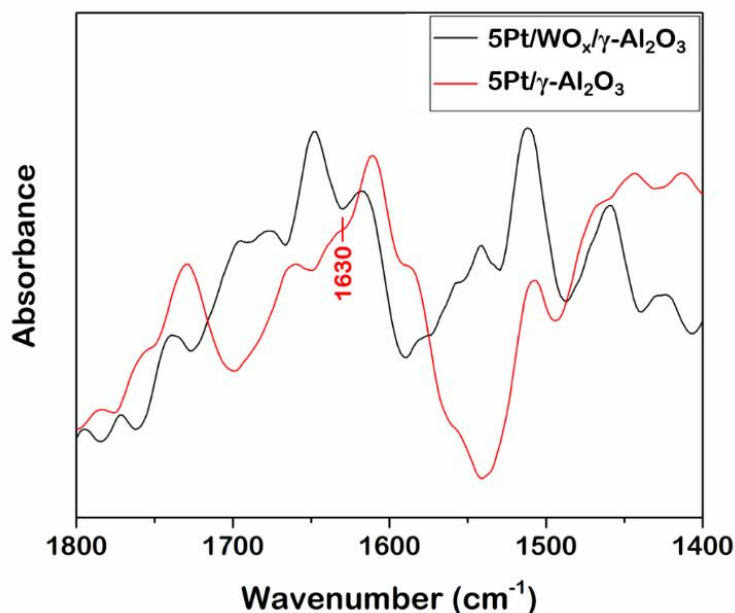
Figure 14 FTIR spectra of used 5Pt/γ-Al$_2$O$_3$ and 5Pt/WOx/γ-Al$_2$O$_3$ catalysts

4.4 Effect of WO$_x$ Existence

Although the deactivation of a solid catalyst such as metal leaching, metal sintering, and coke formation are occurred, the introduction of WO$_x$ can improve both catalytic performances and stability of catalysts.

For catalytic performance, the selectivity of wanted 1,3-PDO on 5Pt/WO$_x$/γ-Al$_2$O$_3$ catalyst is increase beyond 1,2-PDO when WO$_x$ is added on Pt-based catalyst[31-32]. Although 1,3-PDO selectivity on both used catalysts is decreased in the second hydrogenolysis reaction, 1,3-PDO selectivity on used 5Pt/WO$_x$/γ-Al$_2$O$_3$ catalyst is still higher than 5Pt/γ-Al$_2$O$_3$ catalyst.

For stability of deactivated catalyst by coking formation and metal leaching, the catalytic activity of used 5Pt/WO$_x$/γ-Al$_2$O$_3$ is slightly declined, which can be determined by a slight decrement of glycerol conversion utilizing used 5Pt/WO$_x$/γ-Al$_2$O$_3$ catalyst for the second hydrogenolysis compared with 5Pt/γ-Al$_2$O$_3$ catalyst.

From ICP results, these can indicate that the important role of WO$_x$ on 5Pt/WO$_x$/γ-Al$_2$O$_3$ surface can reduce the leaching of Pt metal to the liquid phase. Moreover, the introduction of WO$_x$ on catalysts can reduced coke formation during the hydrogenolysis of glycerol to 1,3-PDO confirmed by TPO and FTIR results.

However, SEM-EDX and XRD results show aggregation of Pt metal to form a larger cluster on both spent 5Pt/γ-Al$_2$O$_3$ and 5Pt/WO$_x$/γ-Al$_2$O$_3$ catalysts.

CHAPTER V

CONCLUSION

5.1 Conclusion

The deactivations of solid Pt-based catalysts are leaching, sintering, and coke formation during hydrogenolysis of glycerol in the liquid phase under mild reaction conditions: 140 °C, 5 bar of initial H_2 pressure and 6 h of reaction time. WO_x on Pt/γ-Al_2O_3 catalyst is not only increase activity, selectivity, and stability of the catalyst, but it is also decrease Pt leaching and coke formation during the hydrogenolysis process.

5.2 Recommendations

5.2.1 Dispersion of Pt metal should be investigated by CO chemisorption to confirm that Pt metal can be moved on catalyst surface during the hydrogenolysis of glycerol.

5.2.2 Py-IR of γ-Al_2O_3 and WO_x/γ-Al_2O_3 catalysts should be studied.

APPENDIX

APPENDIX A

CALIBRATION CURVES

Calibration curves of chemicals such as glycerol, 1,3-PDO, 1,2-PDO, 1-PrOH and 2-PrOH, are done with GC-FID using operating program as reported in Table 2. The mole ratio of chemicals and ethylene glycol as internal standard are prepared and analyzed. Calibration curves of each chemical are plotted between area ratio and mol ratio. Figure 15 – Figure 19 are presented calibration curves of glycerol, 1,3-PDO, 1,2-PDO, 1-PrOH and 2-PrOH, respectively.

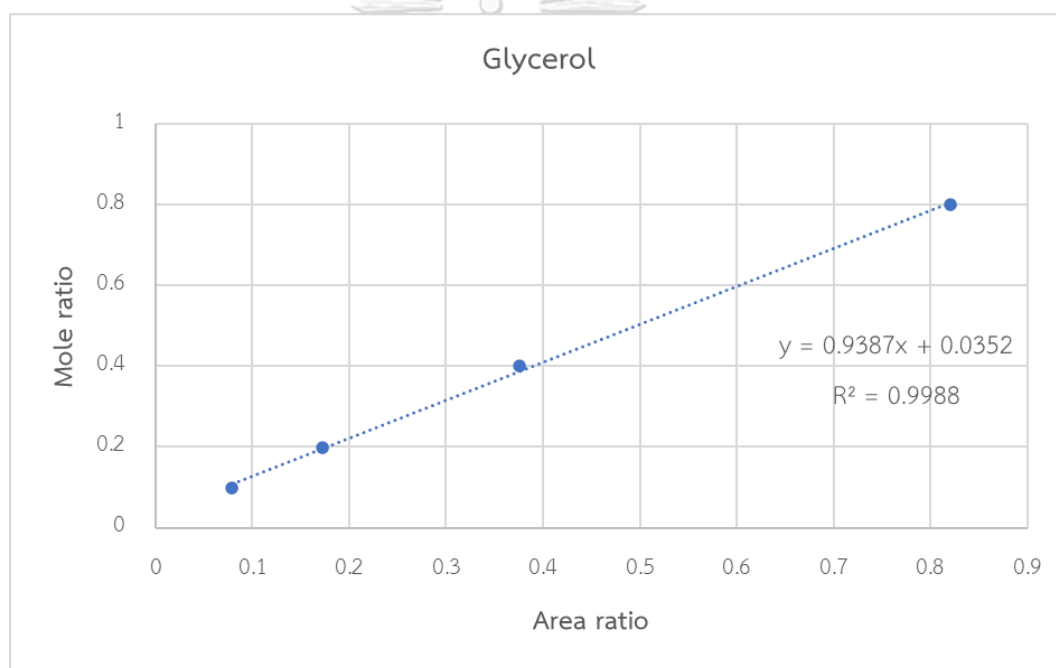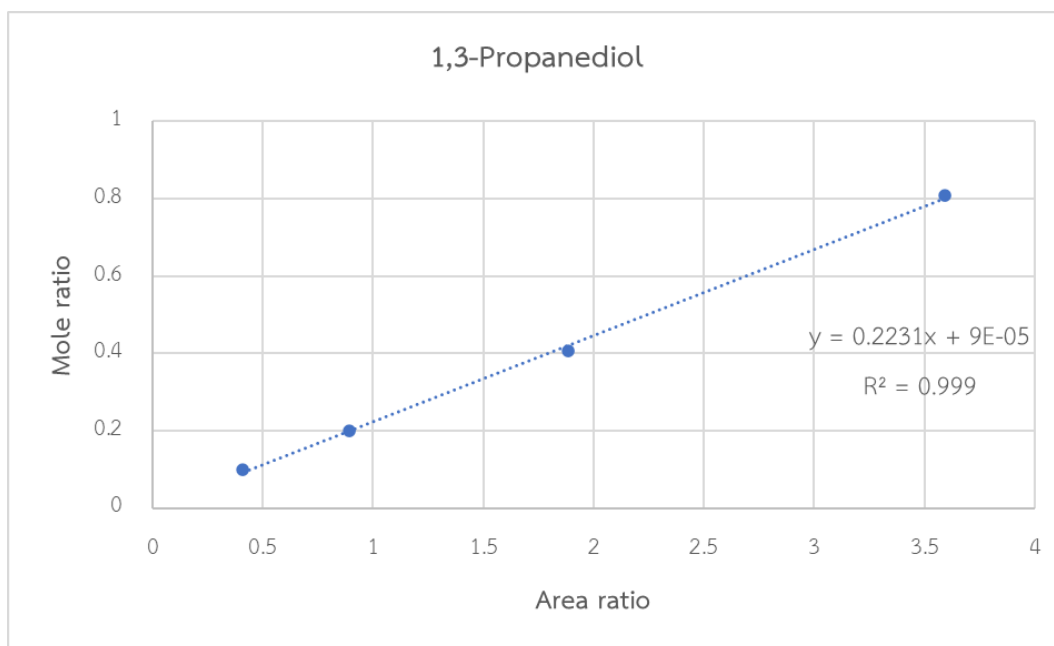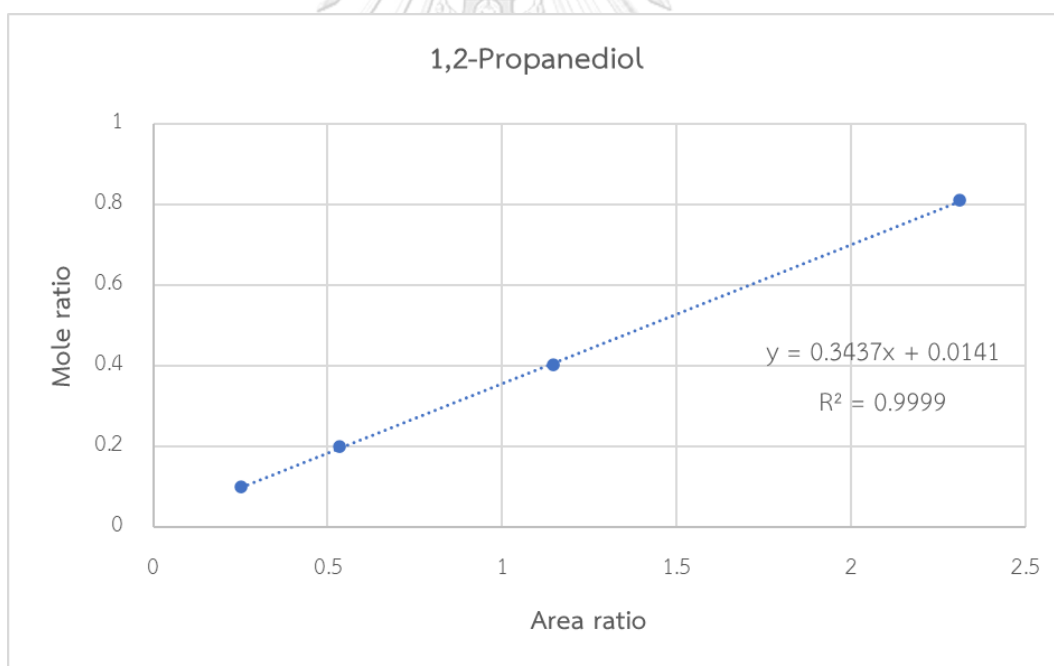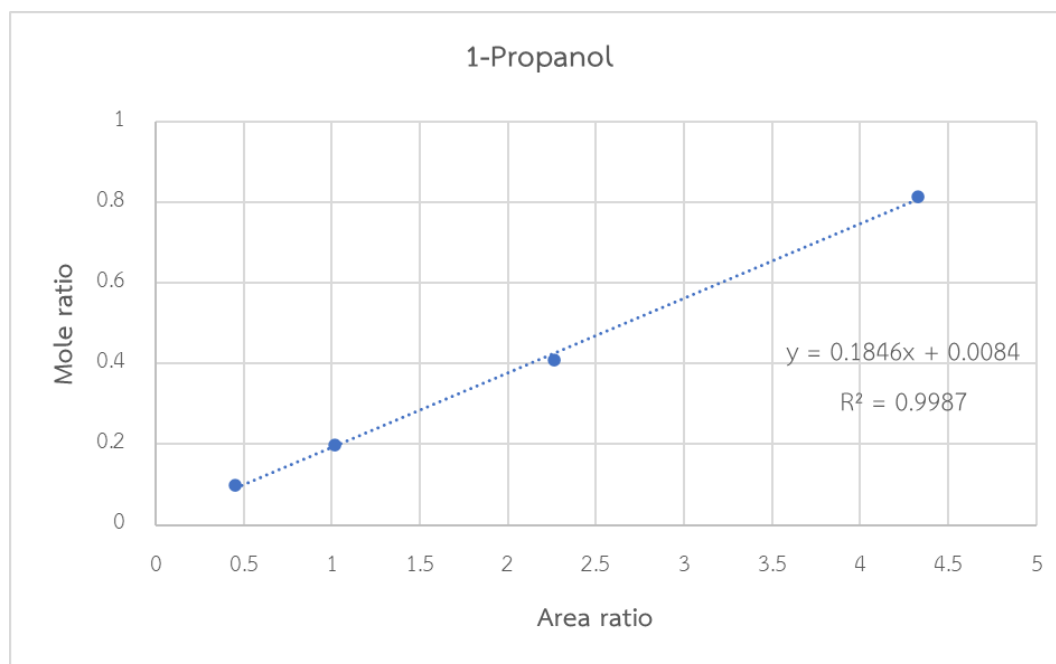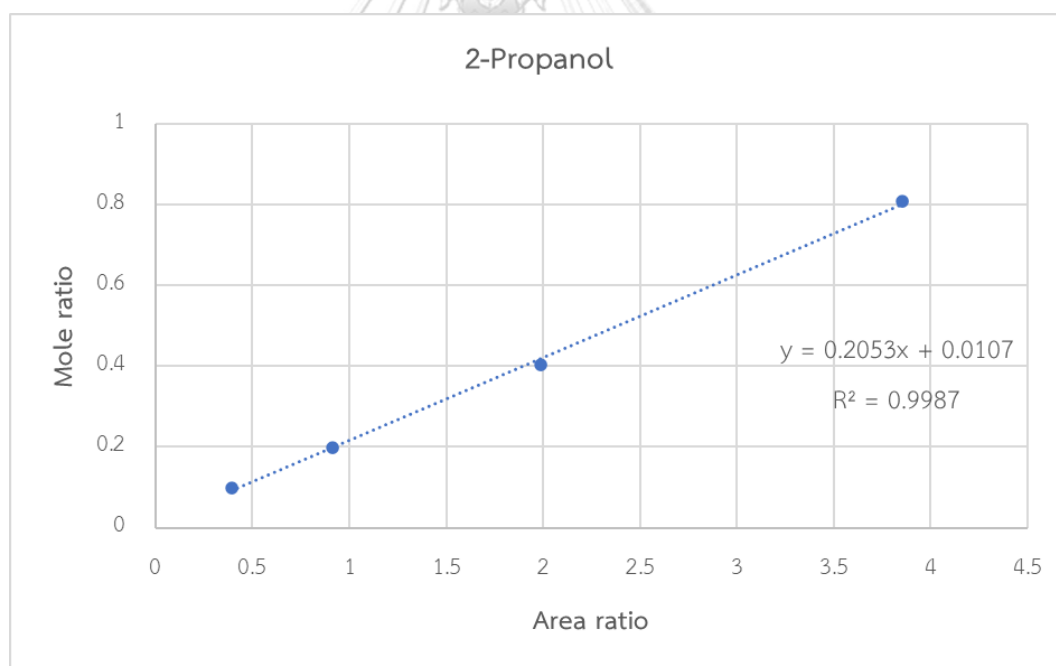

Figure 15 Calibration curve of glycerol

Figure 16 Calibration curve of 1,3-propanediol

Figure 17 Calibration curve of 1,2-propanediol

Figure 18 Calibration curve of 1-propanol

Figure 19 Calibration curve of 2-propanol

APPENDIX B

CALCULATIONS

B.1 Calculation of 5 wt.% Pt metal loading on γ-Al_2O_3 support

Data for calculation:

Sample: 5Pt/γ-Al_2O_3

Precursor: Chloroplatinic acid hydrate ($H_2Cl_6Pt \cdot xH_2O$)   = 409.81 g/mole (38% Pt basis)

Mw of Platinum metal   = 195.084 g/mole

Preparation of 5Pt/γ-Al_2O_3 catalyst

Based on 100 g of catalyst, the compositions of catalyst are follows:

Platinum metal   = 5 g

γ-Al_2O_3 support   = 100 g – 5 g

                                                  = 95 g

For 2 g of γ-Al_2O_3 support

Platinum metal required   = (5/95) x 2

                                                  = 0.1053 g_{Pt}

Platinum metal in precursor (38% Pt basis)   = 409.81 x (38/100)

                                                  = 155.7278 g_{Pt}

Precursor (focusing on Pt metal) required   = (409.81 g_{pre} / 155.7278 g_{Pt}) x 0.1053 g_{Pt}

                                                  = 0.277 g_{pre}

0.277 g of Pt precursor is dissolved in DI water to obtain precursor solution for wet impregnation on γ-Al_2O_3 support.

B.2 Calculation of 10 wt.% WO_x loading on γ-Al_2O_3 support

Data for calculation:

Sample: $10WO_x$/γ-Al_2O_3

Precursor: Ammonium (Meta) tungstate (AMT, $(NH_4)_6H_2W_{12}O_{40} \cdot xH_2O$) = 2956.3 g/mole

(99.99%)

Mw of Tungsten = 183.84 g/mole

Preparation of $10WO_x$/γ-Al_2O_3 catalyst

Based on 100 g of catalyst, the compositions of catalyst are follows:

Tungsten metal = 10 g

γ-Al_2O_3 support = 100 g – 10 g

= 90 g

For 2 g of γ-Al_2O_3 support

Tungsten metal required = (10/90) x 2

= 0.222 g_W

Tungsten metal in AMT (99.99%) = 183.84 x 12 x 0.9999

= 2205.86 g_W

AMT required = (2956.3 g_{pre} / 2205.86 g_W) x 0.222 g_W

= 0.298 g_{pre}

0.298 g of AMT is dissolved in DI water to obtain precursor solution for wet impregnation on γ-Al_2O_3 support.

B.3 Calculation of 5 wt.% Pt metal loading on $10WO_x/\gamma\text{-}Al_2O_3$ support

Data for calculation:

Sample: $5Pt/WO_x/\gamma\text{-}Al_2O_3$

Precursor: Chloroplatinic acid hydrate ($H_2Cl_6Pt \cdot xH_2O$)   = 409.81 g/mole (38% Pt basis)

Mw of Platinum metal   = 195.084 g/mole

Preparation of $5Pt/WO_x/\gamma\text{-}Al_2O_3$ catalyst

Based on 100 g of catalyst, the compositions of catalyst are follows:

Platinum metal   = 5 g

$10WO_x/\gamma\text{-}Al_2O_3$ support   = 100 g – 5 g

                                                    = 95 g

For 2 g of $10WO_x/\gamma\text{-}Al_2O_3$ support

Platinum metal required   = (5/95) x 2

                                                    = 0.1053 g_{Pt}

Platinum metal in precursor (38% Pt basis) = 409.81 x (38/100)

                                                    = 155.7278 g_{Pt}

Precursor (focusing on Pt metal) required   = (409.81 g_{pre} / 155.7278 g_{Pt}) x 0.1053 g_{Pt}

                                                    = 0.277 g_{pre}

0.277 g of Pt precursor is dissolved in DI water to obtain precursor solution for wet impregnation on $10WO_x/\gamma\text{-}Al_2O_3$ support.

APPENDIX C

METAL LEACHING CALCULATION

Metal leaching on catalyst surface into liquid phase of sample from catalytic reaction is investigated using ICP technique. Amount of metal can determine based on the weight of impregnated metal on support.

Data for calculation:

Glycerol 0.36 g	= 0.36 g_{Gly} / (1.11 g_{Gly} mL^{-1})	= 0.324 mL
DI water 11.64 g	= 11.64 g_{water} / (1 g_{water} mL^{-1})	= 11.64 mL
Sample solution	= 0.324 + 11.64	= 11.964 mL

C.1 Metal leaching of fresh $5Pt/WO_x/\gamma-Al_2O_3$ catalyst

Data for calculation:

Amount of Pt metal = 5 wt.%

Amount of W metal = 10 wt.%

Basis: 100 g of catalyst: Pt metal 5 g, W metal 10 g, support 85 g

Based on 0.6 g of catalyst in reaction

W metal	= (10/100) x 0.6	= 0.06 g
Pt metal	= (5/100) x 0.6	= 0.03 g

Amount of W metal from ICP = 1.519 mg/L

Amount of Pt metal from ICP = 0.004 mg/L

Based on: 11.964 mL of sample solution

W metal in sample solution	= (1.519 mg_W / 1000 mL_{sol}) x 11.964 mL_{sol}
	= 0.0182 mg_W
W metal leached	= (0.0182 mg_W / 60 mg_W) x 100%
	= 0.03 %

Pt metal in sample solution	$= (0.004\ mg_{Pt}\ /\ 1000\ mL_{sol}) \times 11.964\ mL_{sol}$
	$= 4.79 \times 10^{-5}\ mg_{Pt}$
Pt metal leached	$= (4.79 \times 10^{-5}\ mg_{Pt}\ /\ 30\ mg_W) \times 100\%$
	$= 0.0002\ \%$

C.2 Metal leaching of used $5Pt/WO_x/\gamma\text{-}Al_2O_3$ catalyst

Data for calculation:

W metal remaining	$= 60 - 0.0182\ mg_W$
	$= 59.9818\ mg_W$
Pt metal remaining	$= 30 - 4.79 \times 10^{-5}\ mg_{Pt}$
	$= 29.9999\ mg_{Pt}$

Amount of W metal from ICP = 0.424 mg/L

Amount of Pt metal from ICP = 0 mg/L

Based on: 11.964 mL of sample solution

W metal in sample solution	$= (0.424\ mg_W\ /\ 1000\ mL_{sol}) \times 11.964\ mL_{sol}$
	$= 0.0051\ mg_W$
W metal leached	$= (0.0051\ mg_W\ /\ 59.9818\ mg_W) \times 100\%$
	$= 0.0085\ \%$

C.3 Metal leaching of fresh $5Pt/\gamma\text{-}Al_2O_3$ catalyst

Data for calculation:

Amount of Pt metal = 5 wt.%

Basis: 100 g of catalyst: Pt metal 5 g, support 95 g

Based on 0.6 g of catalyst in reaction

Pt metal $= (5/100) \times 0.6$ $= 0.03\ g$

Amount of Pt metal from ICP = 0.181 mg/L

Based on: 11.964 mL of sample solution

Pt metal in sample solution $\qquad$ = $(0.181 \text{ mg}_{Pt} / 1000 \text{ mL}_{sol}) \times 11.964 \text{ mL}_{sol}$

$\qquad$ = 0.0022 mg_{Pt}

Pt metal leached $\qquad$ = $(0.0022 \text{ mg}_{Pt} / 30 \text{ mg}_W) \times 100\%$

$\qquad$ = 0.0072%

C.4 Metal leaching of used $5Pt/\gamma\text{-}Al_2O_3$ catalyst

Data for calculation:

Pt metal remaining $\qquad$ = $30 - 0.0022 \text{ mg}_{Pt}$

$\qquad$ = 29.9978 mg_{Pt}

Amount of Pt metal from ICP = 0.055 mg/L

Based on: 11.964 mL of sample solution

Pt metal in sample solution $\qquad$ = $(0.055 \text{ mg}_{Pt} / 1000 \text{ mL}_{sol}) \times 11.964 \text{ mL}_{sol}$

$\qquad$ = $6.58 \times 10^{-4} \text{ mg}_{Pt}$

Pt metal leached $\qquad$ = $(6.58 \times 10^{-4} \text{ mg}_{Pt} / 29.9978 \text{ mg}_W) \times 100\%$

$\qquad$ = 0.0022%

REFERENCES

[1]   L. Bournay, D. Casanave, B. Delfort, G. Hillion, J. A. Chodorge, *Catalysis Today* **2005**, *106*, 190-192.

[2]   A. J. Ragauskas, C. K. Williams, B. H. Davison, G. Britovsek, J. Cairney, C. A. Eckert, W. J. Frederick, J. P. Hallett, D. J. Leak, C. L. Liotta, J. R. Mielenz, R. Murphy, R. Templer, T. Tschaplinski, *Science* **2006**, *311*, 484.

[3]   D. Sun, Y. Yamada, S. Sato, W. Ueda, *Applied Catalysis B: Environmental* **2016**, *193*, 75-92.

[4]   C. A. G. Quispe, C. J. R. Coronado, J. A. Carvalho Jr, *Renewable and Sustainable Energy Reviews* **2013**, *27*, 475-493.

[5]   P. André Cremonez, M. Feroldi, W. Cézar Nadaleti, E. de Rossi, A. Feiden, M. P. de Camargo, F. E. Cremonez, F. F. Klajn, *Renewable and Sustainable Energy Reviews* **2015**, *42*, 415-428.

[6]   J. ten Dam, U. Hanefeld, *ChemSusChem* **2011**, *4*, 1017-1034.

[7]   S. L. Stattman, O. Hospes, A. P. J. Mol, *Energy Policy* **2013**, *61*, 22-30.

[8]   H. Zhang, U. Aytun Ozturk, Q. Wang, Z. Zhao, *Renewable and Sustainable Energy Reviews* **2014**, *38*, 677-685.

[9]   Y. Nakagawa, K. Tomishige, *Catalysis Science and Technology* **2011**, *1*, 179-190.

[10]   M. A. Dasari, M. J. Goff, G. J. Suppes, *Journal of the American Oil Chemists' Society* **2003**, *80*, 189-192.

[11]   R.-R. E. P. N. f. t. s. Century, **2019**.

[12]   OECD, OECD, Paris, **2013**.

[13]   S. García-Fernández, I. Gandarias, J. Requies, F. Soulimani, P. L. Arias, B. M. Weckhuysen, *Applied Catalysis B: Environmental* **2017**, *204*, 260-272.

[14]   H. W. Tan, A. R. Abdul Aziz, M. K. Aroua, *Renewable and Sustainable Energy Reviews* **2013**, *27*, 118-127.

[15]   A. Brandner, K. Lehnert, A. Bienholz, M. Lucas, P. Claus, *Topics in Catalysis* **2009**, *52*, 278-287.

[16]   M. R. Monteiro, C. L. Kugelmeier, R. S. Pinheiro, M. O. Batalha, A. da Silva César, *Renewable and Sustainable Energy Reviews* **2018**, *88*, 109-122.

[17]   M. Schlaf, *Dalton Transactions* **2006**, 4645-4653.

[18]   J. Weitkamp, *ChemCatChem* **2012**, *4*, 292-306.

[19]   A. M. Ruppert, K. Weinberg, R. Palkovits, *Angewandte Chemie International Edition* **2012**, *51*, 2564-2601.

[20]   Y. Wang, J. Zhou, X. Guo, *RSC Advances* **2015**, *5*, 74611-74628.

[21]   C. Montassier, D. Giraud, J. Barbier, in *Studies in Surface Science and Catalysis, Vol. 41* (Eds.: M. Guisnet, J. Barrault, C. Bouchoule, D. Duprez, C. Montassier, G. Pérot), Elsevier, **1988**, pp. 165-170.

[22]   D. G. Lahr, B. H. Shanks, *Industrial & Engineering Chemistry Research* **2003**, *42*, 5467-5472.

[23]   D. G. Lahr, B. H. Shanks, *Journal of Catalysis* **2005**, *232*, 386-394.

[24]   E. P. Maris, W. C. Ketchie, M. Murayama, R. J. Davis, *Journal of Catalysis* **2007**, *251*, 281-294.

[25]   M. A. Dasari, P.-P. Kiatsimkul, W. R. Sutterlin, G. J. Suppes, *Applied Catalysis A: General* **2005**, *281*, 225-231.

[26]   I. Furikado, T. Miyazawa, S. Koso, A. Shimao, K. Kunimori, K. Tomishige, *Green Chemistry* **2007**, *9*, 582-588.

[27]   Y. Amada, Y. Shinmi, S. Koso, T. Kubota, Y. Nakagawa, K. Tomishige, *Applied Catalysis B: Environmental* **2011**, *105*, 117-127.

[28]   M. Chia, Y. J. Pagán-Torres, D. Hibbitts, Q. Tan, H. N. Pham, A. K. Datye, M. Neurock, R. J. Davis, J. A. Dumesic, *Journal of the American Chemical Society* **2011**, *133*, 12675-12689.

[29]   L. Liu, Y. Zhang, A. Wang, T. Zhang, *Chinese Journal of Catalysis* **2012**, *33*, 1257-1261.

[30]   S. Zhu, X. Gao, Y. Zhu, Y. Li, *Journal of Molecular Catalysis A: Chemical* **2015**, *398*, 391-398.

[31]   S. García-Fernández, I. Gandarias, J. Requies, M. B. Güemez, S. Bennici, A. Auroux, P. L. Arias, *Journal of Catalysis* **2015**, *323*, 65-75.

[32]   S. García-Fernández, I. Gandarias, Y. Tejido-Núñez, J. Requies, P. L. Arias,

ChemCatChem **2017**, *9*, 4508-4519.

[33]   N. A. K. Aramouni, J. G. Touma, B. A. Tarboush, J. Zeaiter, M. N. Ahmad, *Renewable and Sustainable Energy Reviews* **2018**, *82*, 2570-2585.

[34]   C. H. Bartholomew, *Applied Catalysis A: General* **2001**, *212*, 17-60.

[35]   I. Gandarias, P. L. Arias, J. Requies, M. B. Güemez, J. L. G. Fierro, *Applied Catalysis B: Environmental* **2010**, *97*, 248-256.

[36]   R. Arundhathi, T. Mizugaki, T. Mitsudome, K. Jitsukawa, K. Kaneda, *ChemSusChem* **2013**, *6*, 1345-1347.

[37]   E. P. PARRY, *Journal of Catalysis* **1963**, *2*, 371-379.

[38]   H. Knözinger, *Handbook of Heterogeneous Catalysis* **2008**, 1135-1163.

[39]   S. S. Priya, V. P. Kumar, M. L. Kantam, S. K. Bhargava, A. Srikanth, K. V. R. Chary, *Industrial & Engineering Chemistry Research* **2015**, *54*, 9104-9115.

[40]   M. Edake, M. Dalil, M. J. Darabi Mahboub, J.-L. Dubois, G. S. Patience, *RSC Advances* **2017**, *7*, 3853-3860.

[41]   S. Feng, B. Zhao, L. Liu, J. Dong, *Industrial & Engineering Chemistry Research* **2017**, *56*, 11065-11074.

[42]   J. ten Dam, K. Djanashvili, F. Kapteijn, U. Hanefeld, *ChemCatChem* **2013**, *5*, 497-505.

[43]   S. Feng, B. Zhao, Y. Liang, L. Liu, J. Dong, *Industrial & Engineering Chemistry Research* **2019**, *58*, 2661-2671.

[44]   W. Zhou, J. Luo, Y. Wang, J. Liu, Y. Zhao, S. Wang, X. Ma, *Applied Catalysis B: Environmental* **2019**, *242*, 410-421.

[45]   T. Aihara, H. Kobayashi, S. Feng, H. Miura, T. Shishido, *Chemistry Letters* **2017**, *46*, 1497-1500.

[46]   H. Zhang, S. Shao, R. Xiao, D. Shen, J. Zeng, *Energy & Fuels* **2014**, *28*, 52-57.

[47]   C.-L. L. Octavio Novaro, and Jin-An Wang, in *Catalytic Naphtha Reforming, Revised and Expanded, Vol. 2* (Ed.: f. M. f. George J. fintos), **2004**, pp. 391-431.

[48]   Merck, https://www.sigmaaldrich.com/, **2020**.

[49]   S. M. Augustine, G. N. Alameddin, W. M. H. Sachtler, *Journal of Catalysis* **1989**, *115*, 217-232.

[50]   J. N. Beltramini, T. J. Wessel, R. Datta, in *Studies in Surface Science and*

Catalysis, Vol. 68 (Eds.: C. H. Bartholomew, J. B. Butt), Elsevier, **1991**, pp. 119-126.

[51]   M. Wolf, N. Raman, N. Taccardi, M. Haumann, P. Wasserscheid, *ChemCatChem* **2020**, *12*, 1085-1094.

VITA

NAME	Poonnapa Limsoonthakul
DATE OF BIRTH	16 April 1996
PLACE OF BIRTH	Songkhla, Thailand
INSTITUTIONS ATTENDED	Bachelor's Degrees in Chemical Engineering
	Faculty of Engineering, Prince of Songkla University
HOME ADDRESS	191 Thumnoonvithi Road, Hatyai Subdistrict, Hatyai
	District, Songkhla Province, Thailand 90110